AN ABSTRACT OF THE THESIS OF

Brian A. Collins for the degree of Master of Science in Nuclear Engineering presented on December 13, 2007.
Title: Experimental Investigation of Condensation Phenomena inside a U-tube Steam Generator

Abstract approved:

Brian G. Woods

Reflux condensation tests examining steam condensation in a PWR steam generator (SG) were conducted at the Oregon State University (OSU) Advanced Plant Experiment (APEX) Test Facility from 2005 through 2007. The experimental data collected will provide a basis to assess TRACE steam generator modeling techniques and assist in development of improved models for condensation and steam generator thermal-hydraulics.

The data collected using the APEX facility is also applied to the EPR reactor design. During a small break loss of coolant accident, reflux condensation may be used in removing the decay heat after reactor shutdown. It has been determined that the decay heat generated after shutdown can be removed by controlling the secondary side pressure to create a temperature difference.

Experimental Investigation of Condensation Phenomena inside a U-tube Steam Generator

By
Brian A. Collins

A THESIS

submitted to

Oregon State University

in partial fulfillment of
the requirements for the
degree of

Master of Science

Presented December 13, 2007
Commencement June 2008

Master of Science thesis of Brian A. Collins presented on December 13, 2007

APPROVED:

Brian G. Woods, Nuclear Engineering

Head of Department of Nuclear Engineering and Radiation Health Physics

---

Dean of the Graduate School

I understand that my thesis will become part of the permanent collection of Oregon State University libraries. My signature below authorizes release of my thesis to any reader upon request.

Brian A. Collins, Author

ACKNOWLEDGEMENTS

I would like to thank the Nuclear Regulatory Commission, office of Nuclear Regulatory Research for their support in funding this project.

I would like to express gratitude to Dr. Brian Woods for the help and guidance given to me through the entire process, John Groome for setting up and running all of the tests using the APEX facility and giving general help and advice, John DeNoma for making the facility modifications, and Teresa Culver for all of the help and support given over the last 3 years.

I would also like to thank my committee members: Dr. Jack Higginbotham, Dr. Debora Pence, and Dr. Henri Jansen.

TABLE OF CONTENTS

TABLE OF CONTENTS (Continued)

TABLE OF CONTENTS (Continued)

TABLE OF CONTENTS (Continued)

List of Figures

List of Figures (Continued)

List of Figures (Continued)

List of Tables

List of Tables (Continued)

Chapter 1 – Introduction

Objective

The primary objective of these experiments is to gain understanding of the phenomena associated with reflux condensation inside the steam generator U-tubes. New pressurized water reactor (PWR) nuclear power plant designs are looking at the possibility of incorporating reflux condensation as a method of heat removal for certain accident scenarios. The main accident scenario is a small break loss of coolant accident (SB-LOCA), and future PWR designs may incorporate reflux condensation as a method of decay heat removal for a SB-LOCA.

To further understand the importance of reflux condensation as a mode of heat removal during a SB-LOCA, the processes and phenomena that occur during a SB-LOCA must be investigated. A PWR operates at high pressures, usually around 15 MPa (2250 psi), to keep the primary side single phase liquid at temperatures around 300 degrees Celsius. The single phase liquid passes through a steam generator which transfers the heat from the primary side and boils water on the secondary side. Figure 1.1 shows the standard primary and secondary systems of a PWR.

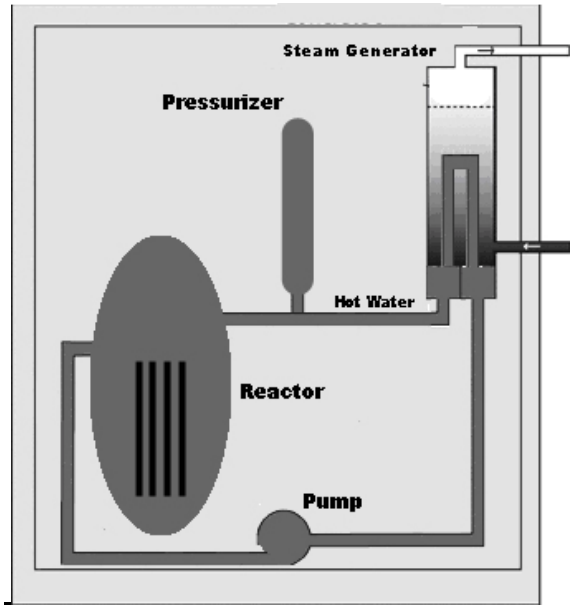

Figure 1.1 – Diagram of Primary Loop of a PWR

During a loss of coolant accident, the pressure on the primary side cannot be maintained. Once the pressure falls below the saturation point of the primary side liquid, some of it flashes to steam. During any accident scenario, the core must stay covered at all times, and emergency systems are designed for this purpose. As soon as an accident scenario is initiated, the reactor shuts down leaving only decay heat to be removed. The amount of decay heat remaining depends on the amount of time at operating power and the type of fuel used, but is usually no greater than 6% of the operating power. For example, a reactor operating at 4500 MW Thermal would have a decay heat no greater than 270 MW immediately after shutdown. As time progresses after shutdown, the amount of decay heat to be removed decreases. Figure 1.2 shows the decay heat curve for reactor shutdown (Todreas & Kazimi, 1990).

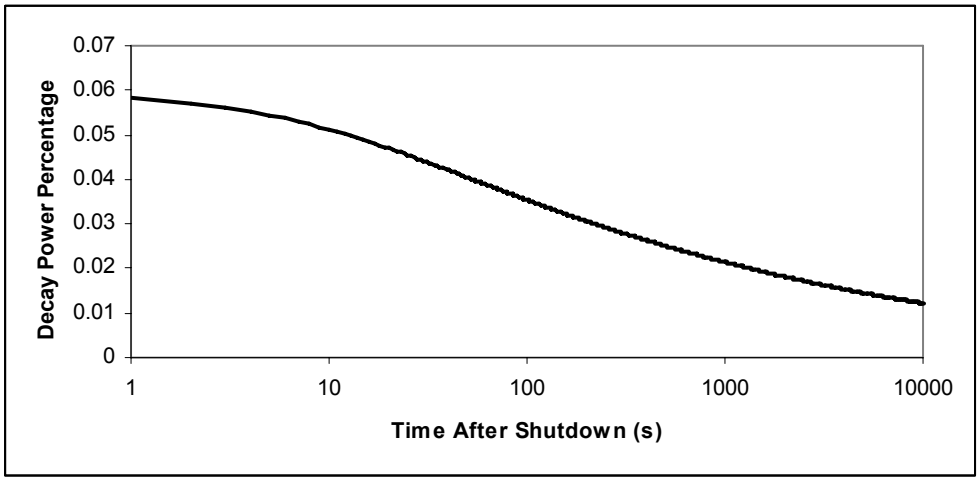

Figure 1.2 – Decay Heat Curve for Reactor Shutdown

After the plant has depressurized there is a two phase mixture of steam and water in the primary side. Figure 1.3 shows a representation of what portion of the core could be under water and where the steam might be.

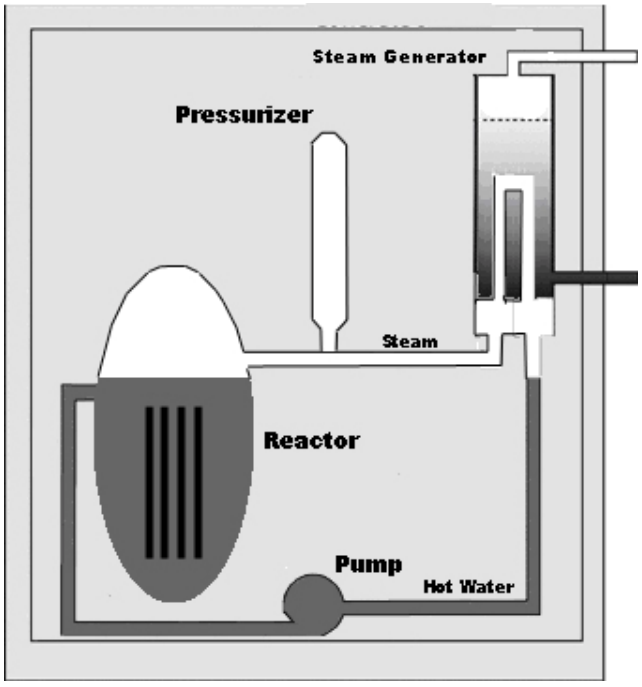

Figure 1.3 – Steam and Water Location after a SB-LOCA

Reflux condensation can take over once the plant is in this phase. The decay heat from the reactor will continue to boil off the liquid inventory, and the steam that is created will flow up into the steam generator. The steam then transfers heat to the secondary side and condenses. The condensate that is formed flows back into the core and replenishes the liquid inventory. This process continues as long as the secondary side of the steam generator serves as a heat sink.

The data provided from these experiments will be used by the NRC to determine the effectiveness of thermal-hydraulic computer codes modeling the reflux condensation phenomenon. Data collected will also be compared with existing data that is similar to the types of experiments run at the Oregon State University APEX facility. The overall research objective is to determine how effective reflux condensation is at removing heat during a severe accident.

Assumptions

During the course of this analysis it has been assumed that there is saturated vapor entering the steam generator U-tubes and saturated liquid on the secondary side of the steam generator. This assumption states that there is no condensate entering the U-tubes during the tests and no steam in contact with the tubes on the secondary side prior to the start of the test.

The control volume for this experiment encompasses the entire steam generator, both the primary and secondary sides, plus the separator tank, catch

tank, and instrumentation. The only thing crossing into and out of the control volume is the steam entering the steam generator U-tubes, the steam exiting through the catch tank and separator tank, and the steam exiting through the secondary side of the steam generator. This gives a boundary condition of only saturated vapor entering or exiting the control volume.

It is also assumed when condensate passes through the valve going into the catch tank; it goes through an isentropic expansion. This assumption states that no energy is lost or gained as the condensate passes through the valve going from high pressure to atmospheric pressure and flashing to steam. This assumption is important because it quantifies the amount of condensate that turned to steam so that it can be used in the mass and energy balances.

Instruments that protrude into the piping (i.e. flow meters, pressure transducers, and thermocouples) do not disrupt or change the steam or condensate flow. Inside the U-tube bundle, all tubes are unplugged and there are no cracks in the tubes that would transfer mass and/or energy to the secondary side of the steam generator directly. It is also assumed the steam separator removes all condensate from the steam flow as it exits the U-tubes, and the final assumption is that the catch tank is not pressurized and is at atmospheric pressure.

Even with the listed assumptions, there are still limitations to this research. The main limitation is lack of instrumentation inside the steam generator and the U-tubes. All of the heat transfer coefficients and film thicknesses are back calculated from known information. The measurement of heat transfer from inside

the 133 U-tubes is limited to only six thermocouples. To fully characterize the steam generator, additional instruments would have to be added. These instruments would include: more thermocouples both to measure the fluid temperature inside and outside the tubes and the wall temperatures of the tubes, additional pressure taps throughout the tube length, and instruments to measure the film thickness inside the tube is also of great importance.

These experiments only model the steam generator as a stand alone component. The system effects, such as total decay heat removal from the core that is possible from reflux condensation is not considered.

The condensation collected is removed from the experiments, so any impact that it may have on the entire system cannot be determined. This still follows the limitation of only showing the phenomena associated with the steam generator. The system wide effects from this process are not considered.

Overview of Chapters

Chapter 2 will provide an overview of the condensation research that has been performed over the last century. It starts with the first condensation experiments performed by Nusselt and ends with reflux condensation experiments in steam generators at an integral systems test facility. The niche that this particular research fills will also be discussed.

Chapter 3 gives information regarding the OSU APEX facility. The chapter mainly deals with the APEX facility and what it was originally designed

for. The systems that are relevant to this particular experiment will be discussed. Chapter 3 also discusses the changes that were made to the facility so that these tests could be performed. As with any large scale facility, there is an inherent uncertainty that can be quantified. This will also be discussed.

All six of the NRC Condensation tests will be discussed in chapter 4. This chapter provides the raw data, such as condensation rates on the uphill and downhill sides of the U-tubes. The experiment procedure and data collection will be discussed, as well as the mass and energy balances.

Chapter 5 discusses the tests in detail and how the results compare to existing literature. The results from these experiments will be compared against similar reflux condensation experiments to see if the data compliments the other research.

The conclusion will discuss future work that could be done to advance the understanding of the topic. This will include modifications to the test facility and the expansion of the test data to cover different flow regimes and phenomena.

Chapter 2 – Literature Review

Condensation

The topic of condensation is a relatively new, but still extensively studied phenomenon. Condensation is the process where a substance changes into a denser phase. This usually is referred to when a vapor or gas is changed into a liquid. There are two ways in which this process can be completed: the first involves the vapor cooling to change to the liquid phase, the second is where the vapor is compressed to the liquid phase. The liquid that is formed is known as condensate and it has been under much investigation for the last century. To understand where this research fits, we will begin with the first condensation experiments, condensation on a flat plate, and work all the way up to reflux condensation in steam generator U-tubes.

Condensation on a Flat Plate

Less than a century ago, Wilhelm Nusselt published his paper "Die Oberflachenkondensation des Wasserdamfes" which analyzed the condensation of steam on a vertical surface. His analysis paved the way for the future work involving the process of condensation. In Nusselt's analysis, he investigated the condensation of steam on a vertical flat plate. The plate was subcooled so the saturated steam would condense on the plate. The condensate that was formed ran down the surface of the plate and formed a film. This film has an impact on many things including temperature and velocity profiles and the overall heat transfer.

However, in this analysis, he assumed a linear temperature profile in the condensation film (Nusselt 1916). Further analysis was conducted and Nusselt's analysis on flat plate condensation was improved.

The next advance in the analysis of condensation came when the linear temperature profile was investigated further. Rohsenow examined the condensate film and determined the temperature profile of the film was non-linear.

While Nusselt's linear approach is sufficient for the majority of flat plate condensation problems, it under predicted the heat transfer coefficient. With the true non-linear profile, a larger heat transfer coefficient would give a larger mass flow rate and a greater film thickness. However, this only has a noticeable effect when the temperature difference of the plate and the vapor is high and the heat of vaporization is low (Rohsenow "Heat Transfer and Temperature Distribution…" 1956).

The analysis presented dealt mainly with a laminar flow regime for the condensate formed on the flat plate. The next logical step was to study the turbulent regime of the condensate flowing down the flat plate. At the top of the plate, as the vapor condenses, the condensate flows down in the laminar regime. However, if the condensation rate is high enough, the flow will enter the turbulent regime. As the condensate flow moves into the turbulent regime, the heat transfer increases. Another important parameter for this problem is the interfacial shear stress between the vapor and condensate. If the interfacial shear stress is significant in the problem, the film will be considered turbulent at lower film

Reynolds numbers. Rohsenow undertook this problem and developed the effect of vapor velocity on turbulent film condensation. (Rohsenow "Effect of vapor velocity on Laminar…" 1956).

Other flat plate condensation references of interest include Sparrow and Gregg 1959, Narain and Kizilyalli, 1991

Condensation in Vertical Tubes

Condensation on a flat plate has been extensively studied and the contributions given above are just a tiny fraction of all the research that has been done on the process. Looking at tube geometry changes the entire process. As the vapor flows up or down the inside of the tube, condensate will form on all of the tube surface area. There have been many different experiments involving vertical tubes including upward and downward vapor flow, laminar and turbulent film condensation, and effects on heat transfer with condensation on vertical tubes.

Laminar Film Condensation

For laminar film condensation in a vertical tube there are two types of flow. First if the steam enters at the top and flows downward, the vapor increases the velocity of the film. For this case Lucas and Moser experimented with vertical tubes with downward vapor flow. They developed a velocity profile for the vapor and condensate and determined the change in heat transfer due to the condensate film. As the condensate flows down the tube walls, the film thickness increases,

and as the film thickness increases, the heat transfer decreases. The experiment also covered horizontal tubes, and when the vertical tubes are compared with the horizontal tubes, it shows an increase of heat transfer for the vertical tubes (Lucas and Moser 1978).

The other type of laminar film condensation in a vertical tube is when the vapor enters from the bottom and flows upward. In this experiment, the vapor was introduced at the bottom of the vertical tube. As the vapor flowed through the tube, condensate formed and would flow down the tube, counter-current to the vapor flow. Seban and Hodgson developed an analytical approach to solve for the behavior of the condensate. In all of their calculations, the condensate had a downward flow, and would flow out of the bottom of the tube. However, since this was a purely analytical exercise, the mixing of the vapor and condensate as they came into contact at the bottom of the tube was not considered. For this exercise, the vapor velocities were not high enough to carry the condensate out of the top of the tube (Seban and Hodgson 1982). With the laminar film condensation investigated, the next logical step was to study the turbulent film condensation.

Turbulent Film Condensation

When the turbulent film condensation was studied on the flat plate scenario, the heat transfer was greater than the laminar case. The focus of the next experiment was to determine the heat transfer coefficient through the turbulent

film as the vapor entered the top of the tube and both the vapor and condensation film flowed downward.

Kim and No developed an elaborate, small scale test facility for this experiment and can be seen in Figure 2.1. 200 kW of electric power were used to produce the vapor for the experiment. The vapor entered the vertical tube and passed through a pool of water to start the condensing of the vapor. By the time the film reached the next section, which was heavily instrumented, the film was fully developed. Thermocouples were used to measure the bulk vapor temperature, the outside wall temperature, and the inside wall temperature. From the data collected with the thermocouples, a temperature profile was determined and the heat transfer through the condensate film was calculated. This experiment setup used pressure varying from .3 MPa to 7.5 MPa.

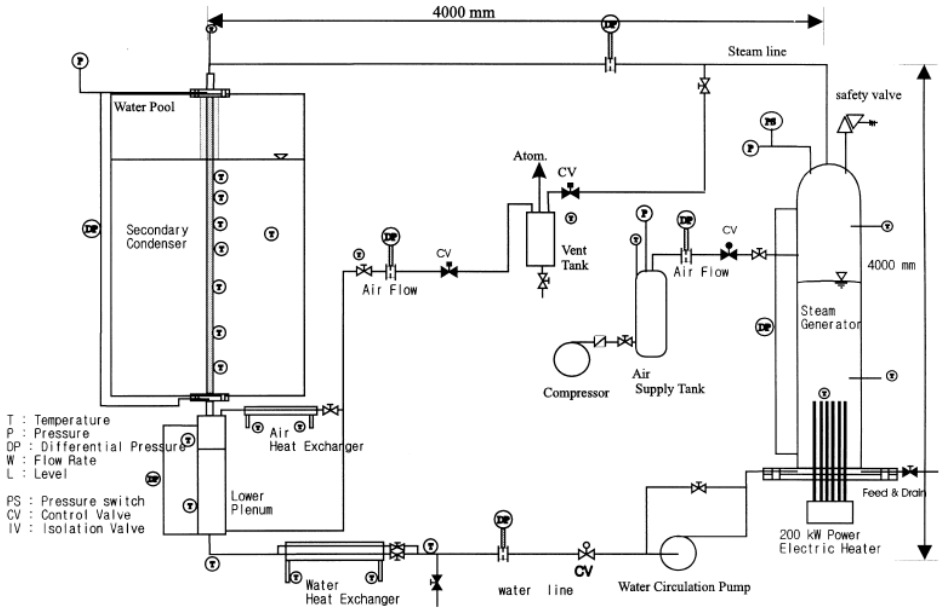

Figure 2.1 – Diagram of Kim & No Test Facility for Turbulent Film Condensation (Used with permission)

The data collected from the experiment was compared with two other experiments. The existing model was determined to be insufficient for modeling the heat transfer, and an improved model was developed. Other similarities and differences can be seen in their experiment write-up (Kim and No 1999). Since the U-tubes are essentially two vertical tubes, one with upward flow and one with downward flow, the next step is to look at the turbulent film regime with an upward vapor flow.

Heat Transfer in Vertical Tubes

A substantial amount of research has been focused on the heat transfer effects associated with the condensation film on the inside of pipes. Most of the experiments discussed earlier had part of their research devoted to the change in heat transfer because of the condensation film. It has been determined that the greater the film thickness, the lower the heat transfer coefficient for the laminar regime. For steam condensation many different phenomena influence the film thickness including: tube length, tube diameter, temperature difference of vapor and tube wall, pressure, vapor direction, and vapor velocity. Each of these parameters will have an effect on the amount of condensation and therefore the condensation film thickness.

Kreidin, Kreidin, and Lokshin designed an experiment to test the heat transfer through the condensate film. Steam flows downward through a center pipe that is surrounded by cold water. Thermocouples line the wall of the inside

tube to measure the wall temperature down the length of the tube. Thermocouples also measure the cooling water temperature down the length of the tube.

From the change in wall temperature and the change in cooling fluid, local heat transfer can be calculated. From their data, it was shown that the local heat transfer through the laminar condensate film decreased further down the tube (Kreidin, Kreidin, and Lokshin 1985).

The next experiment to identify the heat transfer through a condensation film was completed by Borishanskiy, et al. In this experiment, tubes of different diameters were used to develop a correlation between heat transfer and Reynolds Number. They were also attempting to determine where the change from laminar film to turbulent film took place which was denoted as the Critical Reynolds Number. In addition to using different diameters, different pressures and lengths were also used to increase the amount of data so a correlation could be developed that was good for all tube diameters, lengths, and pressures.

This experiment also showed that the addition of a condensate film reduced the amount of heat transferred, but as the film became increasingly turbulent, the overall heat transfer increased as the heat transfer through the condensate film increased. (Borishanskiy, et al. 1981)

Carpenter and Colburn conducted their own experiment to determine the heat transfer in vertical tubes. They developed a correlation dependent on the film Prandtl number and the interfacial shear stress. The correlation that can be seen in Equation 2.1 is valid for interfacial shear stresses between 5 and 150.

$$Nu_{\mathrm{mod}} = 0.043 \cdot \mathrm{Pr}_l^{1/2}\, \tau_i^{*1/2} \qquad (2.1)$$

The applicability of this correlation will be discussed in Chapter 5 (Carpenter and Colburn 1951).

Akers, et al. developed a correlation for the Nusselt number from their experiments that is a function of the steam and film Reynolds numbers, viscosity and density ratios, and the film Prandtl number (Akers, et al. 1959).

$$Nu = 0.026\,\mathrm{Pr}_l^{0.33}\left(\mathrm{Re}_v\left(\frac{\mu_v}{\mu_l}\right)\left(\frac{\rho_l}{\rho_v}\right)^{0.5} + \mathrm{Re}_l\right)^{0.8} \qquad (2.2)$$

Other references for condensation in tubes include Ueda, et al. 1972, Bellinghausen and Renz 1992, Ueda, et al. 1974, Pan 2001, and Sun and Hewitt 2001.

Condensation in U-tubes

The flow geometry of U-tubes can be defined as a vertical tube with upward vapor flow connected to a vertical tube with downward vapor flow. Adding film condensation to the tubes results in condensation flow with counter-current vapor flow connected to condensation flow with concurrent vapor flow. This geometry gives unique flow behavior with both the vapor and the condensate film. Study of condensation in steam generator U-tubes began when it was considered a source of heat removal in nuclear reactors. Many different experiments were developed to quantify what was going on in the U-tubes.

Choi and Lee developed an experiment with a single inverted U-tube to see how vapor, condensate, and air interacted. The experimental setup includes a boiler to produce the steam, the U-tube as the path for the steam to travel, cooling jackets on both the uphill and downhill sides to condense the steam, and a reservoir to collect the excess condensation. There is also an air gap that occupies the top of the U-tube. The volume occupied by the air can be changed by varying the pressure of inside the U-tube. As the vapor condenses, it produces a film of water which can turn into a liquid column of water if enough vapor condenses. Also, the vapor can hold up the liquid column of water inside the tube, an example of this can also be seen in Figure 2.2. It should be noted that these experiments used non-condensable gas; while the experiments conducted using APEX did not.

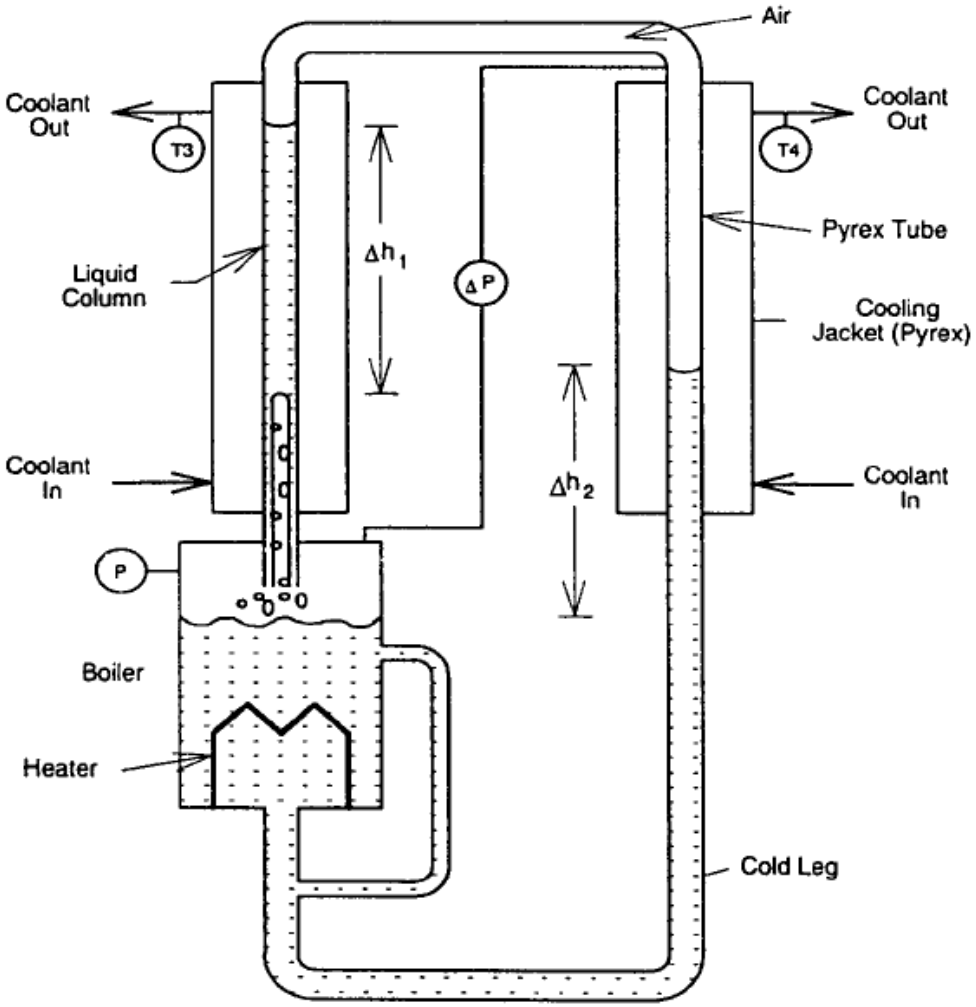

Figure 2.2 – Experimental Setup for Choi and Lee Experiments (Used with permission)

The experiment developed different flow patterns of the liquid column. The three modes were Reflux Condensation, Natural Circulation, and Oscillatory Mode. The three modes had distinct phenomena associated with it. For reflux condensation, the liquid column stayed stationary on the uphill side of the U-tube. Natural circulation mode showed the steam and water flowing over the top bend concurrently into the cold leg. And for the oscillatory mode, the liquid column

would periodically dump over to the cold leg side. The system could change the mode by adjusting the power input into the system. Natural circulation would occur at a higher relative power input, oscillatory would occur at a lower relative power input, and reflux condensation would occur at the lowest relative power input. The experimental data collected was verified against a RELAP5 model of the same experimental setup. The major flow phenomena was modeled using RELAP5. For more information on the outcomes, please refer to the publication (Choi and Lee 1996). The reflux condensation, oscillatory, and natural circulation modes are three distinct types of flow in the U-tube geometry. Out of the three modes, reflux condensation is the mode that the condensation experiments performed at Oregon State University.

Reflux Condensation in U-tubes

Reflux condensation has become an increasingly important phenomenon where small-break Loss of Coolant Accidents (LOCA) are concerned. In a pressurized water reactor, the primary coolant under normal operating conditions is single phase subcooled liquid. However, during a LOCA the plant depressurizes and some liquid in the primary side will boil. All nuclear power plants have safety systems used to keep the core covered during accidents and reflux condensation is a passive process that transfers heat from the core.

In a scenario where the heat cannot be removed from the coolant, the coolant will begin to boil and the steam will travel into the steam generators. As

the steam flows up into the U-tubes, some of it will condense on the tube walls and the condensate film that is formed will flow back down to the core due to gravity. Banerjee, et al. designed an experiment to determine the different parameters that affect reflux condensation in U-tubes.

Vapor enters the tube from the bottom and condenses. There is a two phase mixture up to a specific point which is determined by parameters such as steam velocity, pressure, mass flow rate, etc. There is also a single phase liquid region that stays in the uphill side of the tube. The length and height of the liquid region is also determined by the same parameters that affect the two phase region (Banerjee, et al. 1983).

An experiment that involves a single tube will react differently than a multi-tube setup. The use of an actual steam generator will provide different results due to the many tubes of different lengths for the steam to travel through. Liu set up a reflux condensation experiment using the Institute of Nuclear Energy Research (IIST) integral system test facility to perform many reflux condensation tests. Figure 2.3 shows the schematic of the test facility.

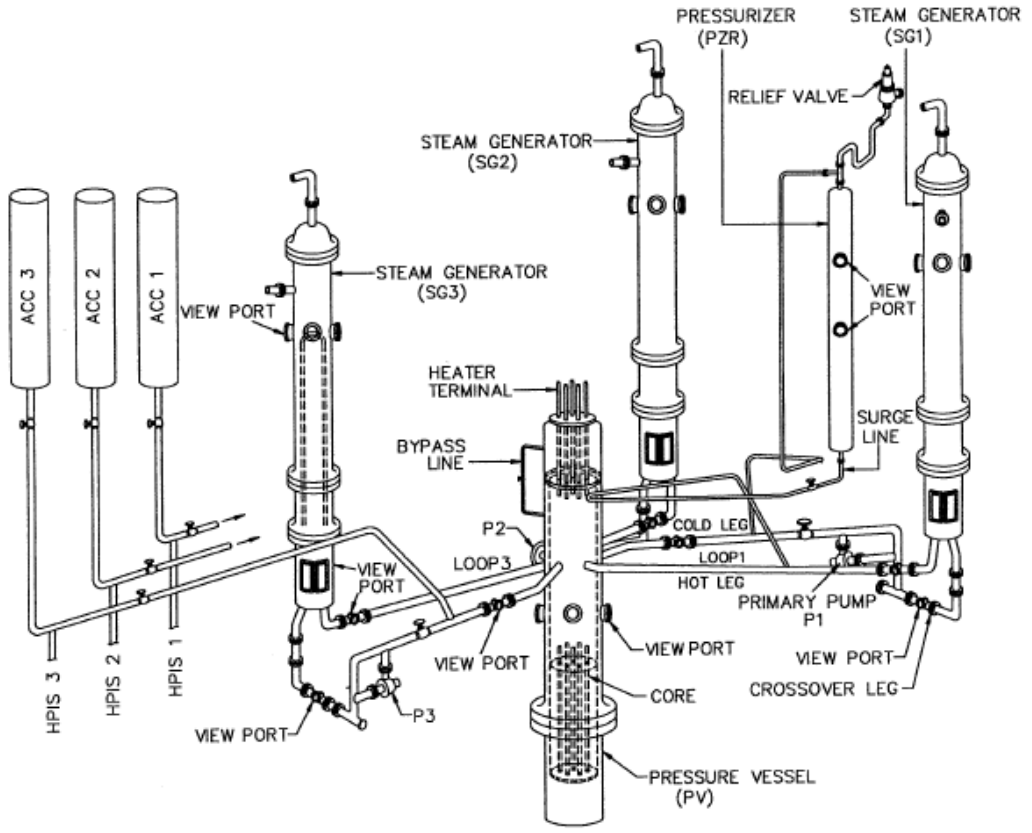

Figure 2.3 – Schematic of the Institute of Nuclear Energy Research Test Facility (Used with permission)

The experiment provided results for a variety of test conditions. The data that was recorded included temperatures, mass flow rates of steam and condensate, water levels in different components of the facility, and pressures throughout the system. The goal of this experiment was to provide data on how much heat could be removed from the system using the reflux condensation inside the steam generators. The effects in the steam generator were documented as how they related to the system as a whole. The reflux condensation, oscillation, and natural circulation modes were also studied in the experiments and comparisons made to the FLECHT SEASET tests show similar behaviors (Liu 2000).

Another facility conducting system wide experiments on condensation phenomena using U-tube steam generators was FLECHT SEASET. The Full Length Emergency Cooling Heat Transfer Separate Effects And System Effects Test facility conducted single phase, two phase, and reflux condensation tests to determine the heat transfer abilities of the steam generators. More analysis of the FLECHT SEASET tests will be covered in Chapter 5 (FLECHT SEASET 1984).

Other research involving reflux condensation includes Girard and Chang 1992, and Jeong et al. 1998.

APEX Facility Tests

The tests performed at the OSU Advanced Plant Experiment facility closely resemble the ones that Liu performed at the IIST facility, however there are differences in the tests performed at the two facilities. The IIST facility had three intact steam generators for their tests and the entire system was modeled in the tests. The tests performed using the APEX facility were looking at the effects in a single steam generator that was not connected to the system. Dry steam was directed into the steam generator hot leg and flowed through.

Another big difference is that the condensate that was formed on the inside of the tubes was collected and removed from the system on both the uphill and downhill sides in the APEX tests. Many other experiments allowed the condensate to recirculate. The data collected using the APEX facility will give needed information about the condensation effects in a single steam generator. The

information will be used to benchmark computer codes against the data collected, and to investigate whether reflux condensation is sufficient to remove decay heat after shutdown from a SB-LOCA.

Chapter 3 – Materials and Methods

APEX Description

The Oregon State University Advanced Plant Experiment (APEX) is a world class facility originally designed to assess the safety systems of the Westinghouse designed Advanced Passive 600 and 1000 Pressurized Water Nuclear Power Plants.

APEX is a thermal-hydraulic, integral system test facility originally built to model long term accident scenarios for the AP-600 plant. After certification of the AP-600 plant was complete, APEX was modified to model the AP-1000. In all, 75 system tests were performed for Westinghouse and the Nuclear Regulatory Commission. The information contained in this chapter is limited to systems relevant to the current experimental program. For a more detailed description of the APEX Facility, please refer to Reyes and Groome (Reyes and Groome 2003).

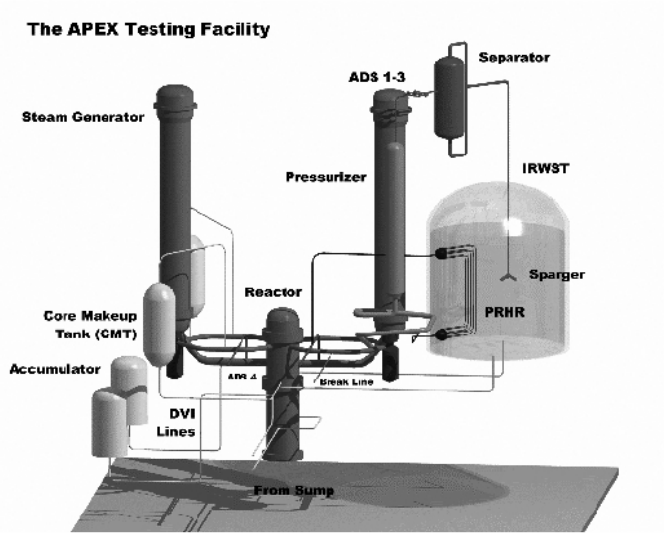

Figure 3.1 – APEX Facility Layout

Figure 3.1 shows the APEX facility layout which models the two-loop AP-1000 PWR. Additional safety systems, such as the IRWST, accumulators, and core makeup tanks, were designed to make the plant passively safe in the event of an accident.

Figure 3.2 shows an elevation view of the APEX reactor coolant system. The reactor coolant system includes the reactor vessel, four cold legs, two hot legs, two steam generators, a pressurizer and four reactor coolant pumps.

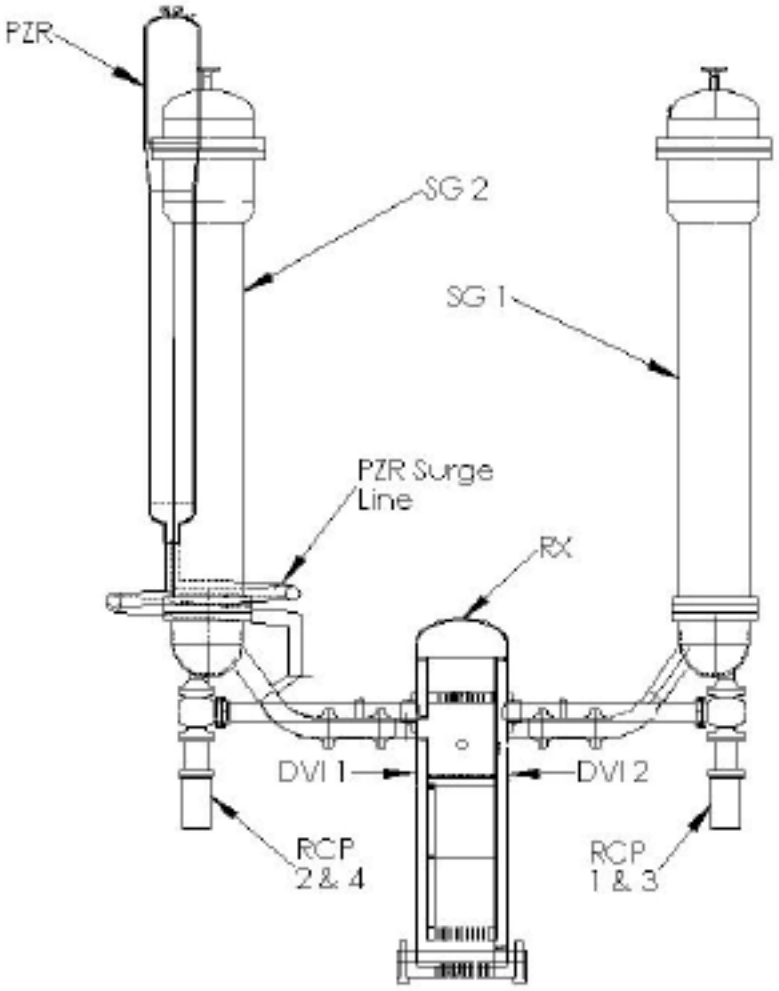

Figure 3.2 - Elevation View of Reactor Coolant System

The reactor vessel is heated electrically by 48 heater rods to produce a maximum power of 1 MW. Nominally, cold water enters through four cold legs into an annular downcomer region. The cold legs are 3.5 inch diameter schedule 30 stainless-steel pipe. The cold water then goes through the lower plenum and then through the core. The water is then heated by the electric heater rods as it passes through the heater rod bundle. After being heated, the water leaves the reactor out of two hot leg nozzles. Figure 3.3 shows the reactor vessel cross section view.

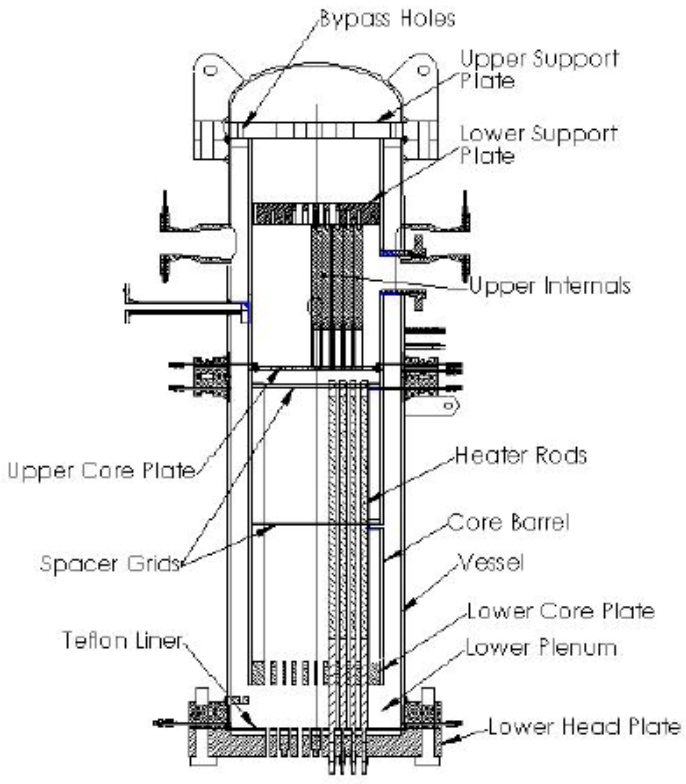

Figure 3.3 – Cross Section View of Reactor Vessel

After leaving the vessel, the water travels through the hot legs into the steam generators. The hot legs are made of 5 inch diameter schedule 30 stainless-steel pipe. Attached to one of the hot legs is the pressurizer. The function of the pressurizer is to maintain the primary loop at a given pressure. Four heaters in the pressurizer are used to regulate the pressure. Figure 3.4 shows the illustration of the pressurizer geometry. The lower portion is constructed out of 12 inch schedule 40 stainless-steel pipe and the top portion is constructed out of 16 inch schedule 30 SS pipe.

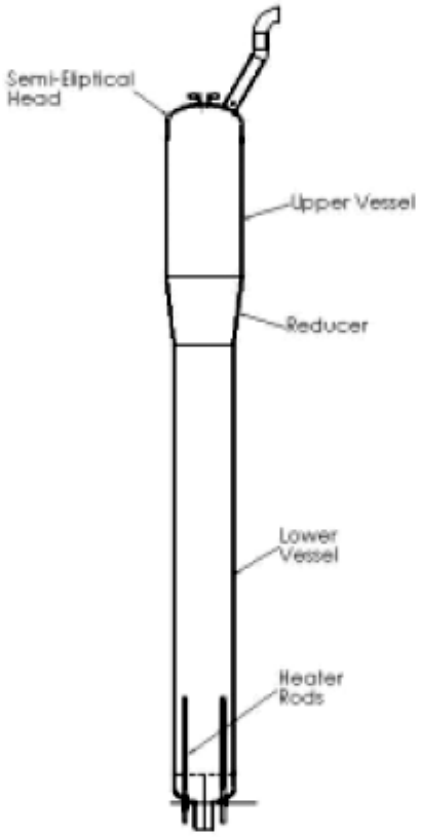

Figure 3.4 – Illustration of Pressurizer Geometry

There are two steam generators in APEX, one for each hot leg. Each is instrumented and simulates a Westinghouse Delta-75 steam generator. After entering the steam generator through the lower head, the water travels through 133 U-tubes (0.687 inch outside diameter, 0.607 inch inside diameter). Figure 3.5 shows the steam generator components

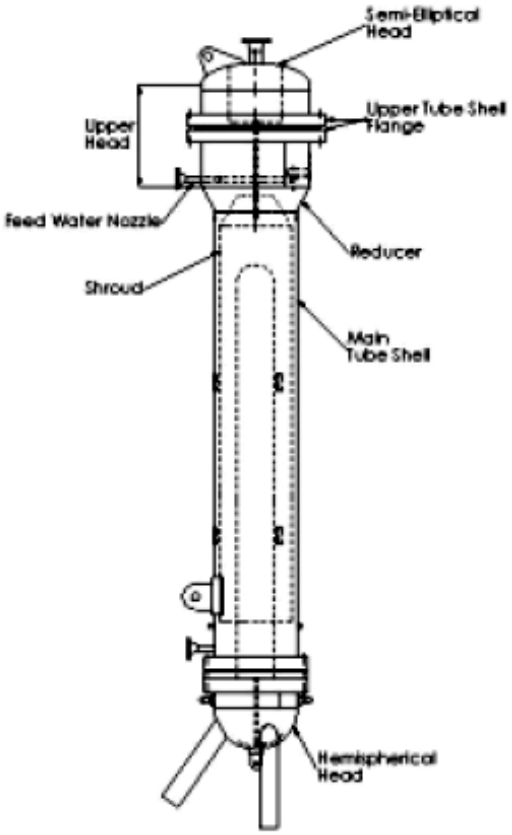

Figure 3.5 – Steam Generator Components

After traveling through the U-tubes, the water reaches the lower head of the steam generator and then goes through the reactor coolant pumps. There are four

variable speed reactor coolant pumps. Two are attached to the lower head of each steam generator. The outlet of each pump is connected to a cold leg, and each pump can be programmed to simulate a specific flow. Each pump has a maximum output of 320 gallons per minute at 420°F.

Facility Modifications

Several modifications were made to the APEX facility in order to complete the reflux condensation testing program. These changes can be seen in Figure 3.6 and are discussed below.

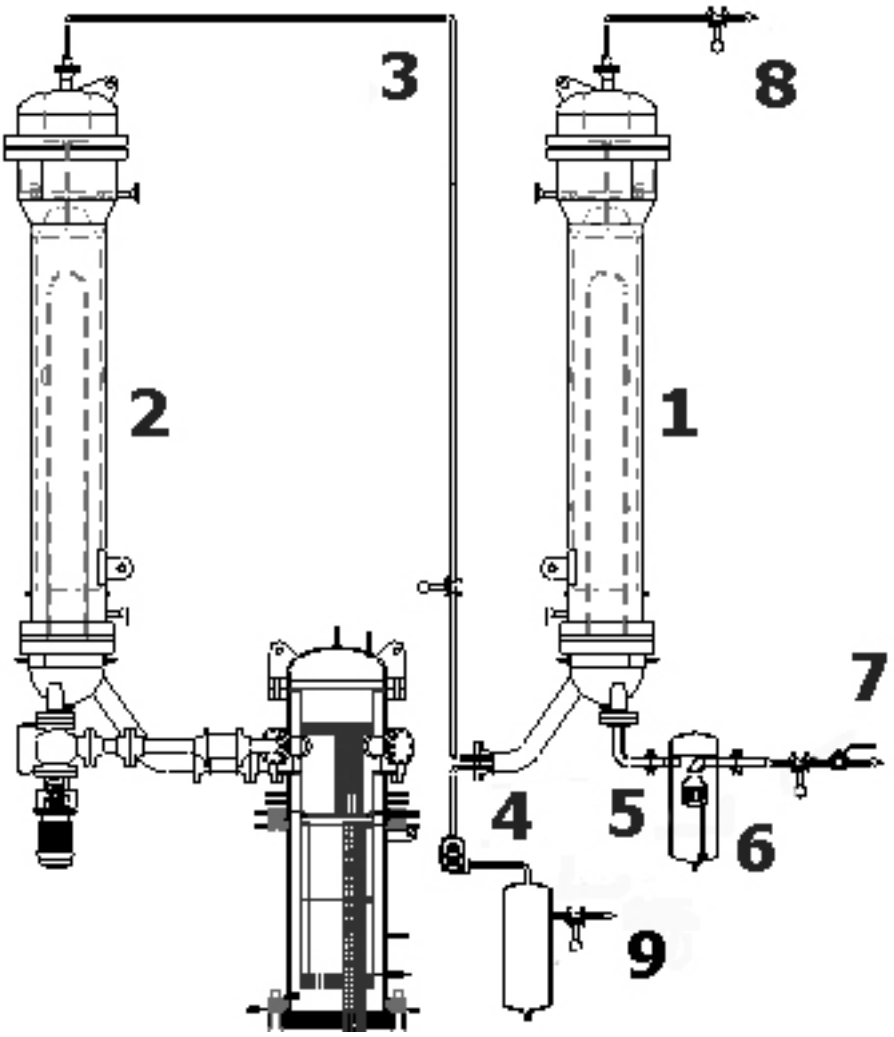

Figure 3.6 – Changes made to APEX for Reflux Condensation Tests

The numbers represent the description of the components in Figure 3.6

1. Steam Generator #1 was removed from the primary looping system by disconnecting the hot and cold legs from the reactor vessel.
2. Steam Generator #2 remains connected to the reactor vessel and produces the dry steam that flows through the Steam Generator #1 U-tubes during the tests.
3. In the original AP-600/1000 configuration, the steam produced from the steam generators was vented directly to atmosphere. In order to use this steam for the testing purposes, the steam line was modified so that the dry steam travels to Steam Generator #1. A hand operated valve controls the amount of steam leaving Steam Generator #2. A volumetric flow meter measures the volume of steam and a pressure gauge measures the pressure. From these two instruments a mass flow rate can be obtained. The steam travels through a 2 inch diameter pipe between the steam generators and goes through two 90° turns before entering Steam Generator #1.
4. The dry steam enters the hot leg of Steam Generator #1. The hot leg was disconnected from the primary system, and the hot leg of the reactor was flanged off. A flange was drilled out to allow the steam pipe to enter the hot-leg, or uphill, side of the U-tubes. Another hole was drilled to allow the condensed steam to flow out of the U-tubes into the catch tank.
5. The steam travels through the U-tubes where some of it is condensed, and leaves through the cold leg or downhill side of the steam generator. Under AP-600/1000 configuration there are two reactor coolant pumps coming

out of the two cold legs that pump the primary coolant water back into the reactor. For this experiment, the reactor coolant pumps were removed, one of the cold leg exits from Steam Generator #1 was flanged off, and the remaining cold leg was modified to allow steam and condensation to flow out of Steam Generator #1.

6. The steam and condensation mixture flows into the separator tank. The separator tank is a cyclone separator designed to remove all of the condensate from the steam flow. The condensation that was removed collects at the bottom of the separator. The separator is at steam pressure, which is determined by the test being performed, and a level measuring instrument is used to determine the condensate level in the separator.
7. After leaving the separator, the steam flows through another pressure gauge and volumetric flow meter. These instruments measure the outlet volumetric flow rate and pressure of the steam as it leaves the separator. Next the outlet steam flows through another valve used to set the outlet flow of the steam. After flowing through the valve, the steam is vented into the break separator and then to atmosphere.
8. As the steam flows through the U-tubes, it transfers heat to the secondary side of Steam Generator #1. Since the water in the secondary side is considered saturated liquid, the heat flowing into the secondary side boils the liquid. A motor operated valve controls the amount of steam leaving

the secondary side. The steam travels through a pressure gauge and a volumetric flow meter before venting to atmosphere.

9. The condensate that is formed as the steam flows through the hot-leg, or uphill side of Steam Generator #1 collects into the catch tank. The tank is at atmospheric pressure and has a level measuring instrument so that the level of the condensate is known. For NRC Condensation Tests 1, 2, & 3, a float valve was installed upstream from the catch tank to allow condensate to flow into the tank without releasing steam. For NRC Condensation Tests 4, 5, & 6, a ball valve was used and a constant steam flow out of the catch tank was measured. Before being vented to atmosphere, the steam flowing through the catch tank is measured by a volumetric flow meter.

Table 3.1 below shows the Catch Tank and Separator Tank diameter, maximum liquid height, and maximum volume. Using level instruments DP-217 and DP-219 the volume of condensation can be determined.

Table 3.1 – Separator and Catch Tank Specifics

Component	Diameter	Max Liquid Height	Max Volume
Separator Tank	11.938 in	22 in	1.425 ft^3
Catch Tank	11.938 in	22 in	1.425 ft^3

The separator and catch tanks are constructed out of 12 inch outside diameter stainless steel. They were pressure tested to 400 psig to ensure that they could handle the maximum pressure of the APEX facility. Each of the tanks is insulated to reduce the amount of heat transferred to the surroundings.

Both the separator and catch tanks need to be drained between each step of the test due to the volume of condensate collected in the tanks. To prevent flashing at the outlet, the condensate separator drains into the break separator. Since the catch tank is at atmospheric pressure, it drains straight to the floor drain.

A list of tag names and descriptions for all of the instruments used for the modified APEX tests can be seen in Table 3.2. These are the instruments used for data analysis.

Table 3.2 – List of APEX Instruments

Components Used in NRC Steam Condensation Tests 1-6	
Tag Name	Description
DP-211	Steam Generator #1 Short Tube Entrance Losses
DP-213	Steam Generator #1 Long Tube Exit Losses
DP-217	Separator Tank Level (in)
DP-219	Catch Tank Level (in)
FVM-001	Steam Outlet Volumetric Flow Rate (cfm)
FVM-002	Steam Inlet Volumetric Flow Rate (cfm)
FVM-003	Steam Out SG Secondary Side Volumetric Flow Rate (cfm)
FVM-004	Steam Out Catch Tank Volumetric Flow Rate (cfm)
LDP-301	Steam Generator #1 WR Uncompensated Water Level (in)
LDP-302	Steam Generator #2 WR Uncompensated Water Level (in)
LDP-303	Steam Generator #1 NR Uncompensated Water Level (in)
LDP-304	Steam Generator #2 NR Uncompensated Water Level (in)
PT-002	Steam Out SG Secondary Side Pressure (psig)
PT-004	Steam Inlet Pressure (psig)
PT-107	Reactor Upper Head Pressure (psig)
PT-301	Steam Generator #1 Pressure (psig)
PT-302	Steam Generator #2 Pressure (psig)
PT-501	Steam Outlet Pressure (psig)
PT-604	Pressurizer Pressure (psig)
TF-211	Outlet Short U-tube Thermocouple (F)
TF-213	Outlet Long U-tube Thermocouple (F)
TF-215	Inlet Short U-tube Thermocouple (F)
TF-217	Inlet Long U-tube Thermocouple (F)
TF-301	Steam Generator #1 Steam Temperature (F)
TF-305	Steam Generator #1 Downcomer Hotleg Side Temperature (F)
TF-307	Steam Generator #1 Downcomer Coldleg Side Temperature (F)
TF-310	Steam Generator #2 Steam Temperature (F)

Mass and Energy Balances

Mass and energy balances are conducted to make sure the experiment is following the expected plan. For these experiments, condensate could be entrained in the steam generator tubes. Conducting mass and energy balances helps identify potential problems during the tests to make sure the designed experiment is followed.

Due to the data measurement process random errors are present and systemic errors may be present. When many measurements are taken, the random errors are usually evenly distributed around the true mean. These errors are dealt with by taking many measurements and averaging the values. The systemic errors can be harder to detect and usually favor being too high or too low. The error bars on the graphs represent errors due to instrument uncertainty; refer to Appendix A for the facility uncertainty calculations for each test.

For each step in all of the tests, a mass and energy balance was completed. Figure 3.7 shows the mass balance value with the associated facility uncertainty for the test and step. Figure 3.8 shows the value and uncertainty for the energy balance. Step 1 of each test was used to determine the ambient heat losses of the system.

As the graphs show, the mass balance favors a positive error while the energy balance favors a negative error. This is evidence of a systemic error in the system. The likely cause is an instrument that is measuring with a bias. From the data collected, the instrument, or instruments, that most likely have a bias that

would affect the mass and energy balances are the flow meters or pressure transducers.

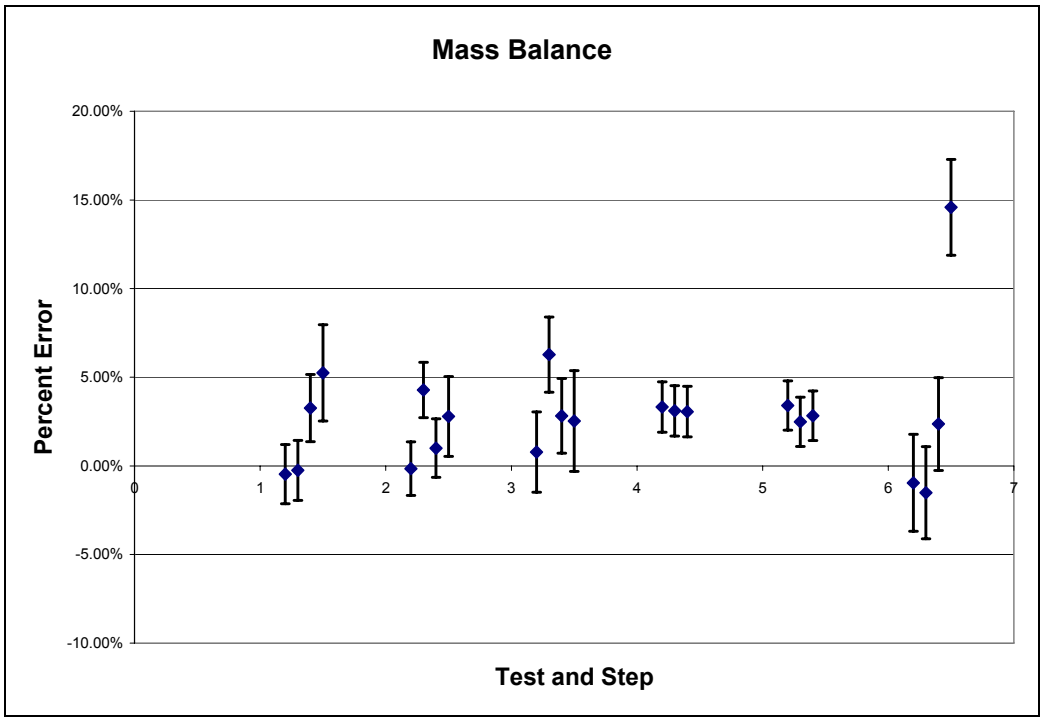

Figure 3.7 – Mass Balance for Each Test and Step

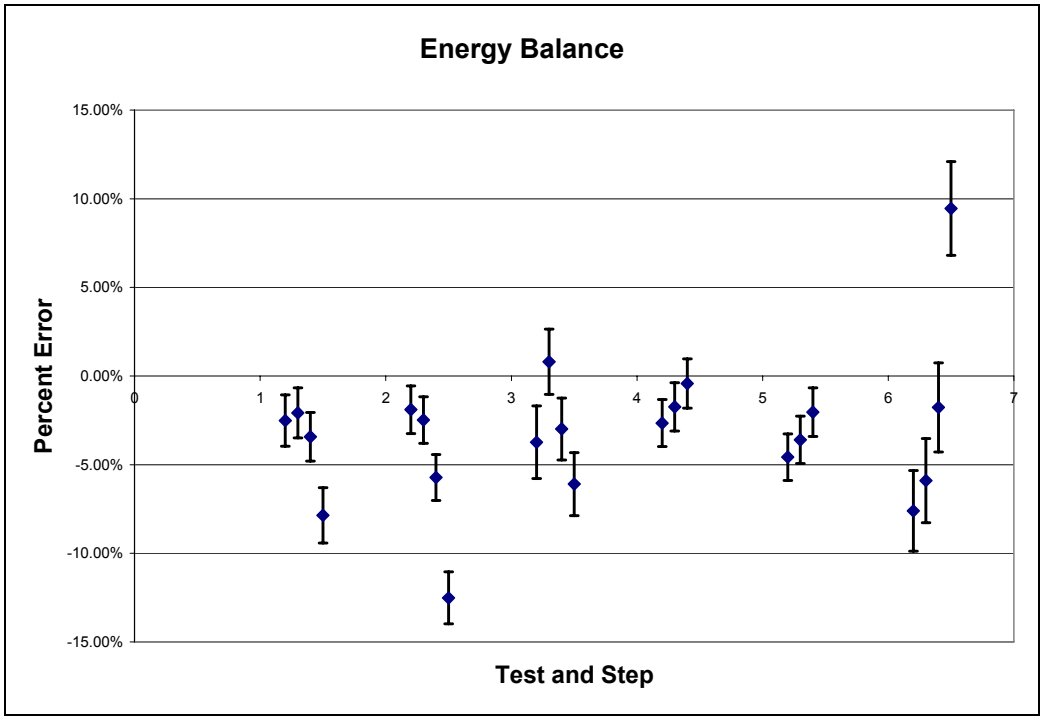

Figure 3.8 – Energy Balance for Each Test and Step

When looking at the mass balance all but three are less than five percent error, and all but one are less than ten percent error. Test 6 Step 5 shows an error of 14.58%. Carry-over of condensation was seen during this step. This higher error is possibly attributed to the separator not collecting all of the condensate due to the higher velocity of the steam and condensate mixture or holdup of condensate in the U-tubes, other sources can be instruments operating near their upper range value, for example, the inlet and outlet volumetric flow meters were operating near their upper range values. Other than that step every other test and step is well within the ten percent error region.

The energy balance shows a similar trend. Eight of the steps have an energy balance error greater than five percent, and only one has an error of more

than ten percent. For a more detailed calculation of the mass and energy balances for each of the tests and subsequent steps, refer to Appendix B.

Experiment Procedure

Each test that is run using the APEX facility follows a specific test procedure for quality control purposes. The test procedure includes plant startup procedures, equipment locations, test specific materials or procedures, and plant configuration.

For each of the six tests, the same startup procedure was followed. This included a visual check of the plant to identify that modifications matched the test being performed, the power up of the facility and operating instruments, and an instrument check to determine the conditions of the facility.

After the facility has been approved for test startup the initial heating and pressurizing of the plant begins. Depending on the pressure of the test, this can take between three to six hours. The temperature of the liquid water in the primary loop is always twenty degrees subcooled to prevent boiling while the plant is being pressurized.

When the facility has reached the pressure determined by the test being performed a final check list is performed. This checklist includes valve position verification, controller set-point verification, pump location verification, and plant software verification. Once all of the pre-test steps have been performed, the facility is ready for the test.

The test actuation begins with the pressing of the test button trigger, which initiates the data logging for the data acquisition system. The start time for the test is recorded. Each test has four or five steps associated with it. These steps have a pre-determined inlet, outlet, and secondary energy associated with them. For each test, Step 1 was used to determine the ambient heat loss of the system by having the inlet fully open and the outlet and secondary closed. For NRC-COND-001, NRC-COND-002, and NRC-COND-003 the secondary side was opened to approximately 100 kW of energy out for Steps 2, 3, and 4 and was fully closed for Step 5. The outlet valve was varied in position for each of the steps to let the pre-determined amount of energy out of the system. NRC-COND-004 and NRC-COND-005 only had four total steps for each test and NRC-COND-006 had five steps.

After all of the steps for the particular test had been completed, the test button trigger was pressed again to stop the data recording and the facility went through the shut-down procedures.

Data Collection

The APEX facility has 622 instrument channels used to record the behavior of the plant. There are 9 different types of channels which include:

- Thermocouples (TF, TH, TW) – Used to measure fluid, heater, and wall temperatures
- Magnetic Flow Meters (FMM) – Used to measure single phase liquid flows

- Vortex Flow Meter (FVM) – Used to measure single phase vapor flows
- Pressure Transducers (PT) – Used to measure static pressures inside tanks and pipes
- Differential Pressure (LDP, DP) – Used to measure liquid levels in tanks and pipes, DPs can be used to measure pressure drop
- Heated Phase Switches (HPS) – Used to determine the fluid phase inside the piping
- Load Cell Transducers (LCT) – Measures liquid mass inside the IRWST and sumps
- Heater Power (KW) – Power to the core is measured with four power meters
- Level Transducers (LT) – Used to measure reactor vessel collapsed liquid level (Reyes and Groome 2003)

For the purpose of these experiments the following types of instruments are used for data collection and analysis: thermocouples, vortex flow meters, pressure transducers, and differential pressure instruments. The other instrument types are still used for the operation of the plant; however the data is not used for analysis.

The instrumentation used for this experiment has an upper and lower limit. For this experiment it is assumed that instruments reading from -1 to ~2 are reading below their lower level limit and assumed zero. This prevents false readings when the instrument is measuring at or near its lower limit.

The inside and outside diameter of the U-tubes has zero error associated with the measurement. Justification for this assumption is that there are 133 U-tubes used in these experiments. Assuming a random error in the manufacturing process giving both larger and smaller diameters, the error will be averaged to zero because of the number of tubes involved. If there was a small amount of tubes or even a single tube, this assumption might not be valid.

The APEX data acquisition system (DAS) records the data from each of the instruments to a single database. The DAS acquisition frequency is 1 Hz. After all of the data has been collected, a program written by Oregon State University exports it to ASCII text format. Individual instruments can be selected during the export process; and when complete, the ASCII file is imported into Excel for analysis.

Chapter 4 – Data and Analysis

Chapter 4 discusses the data collected from all six of the steam condensation tests. Each of the tests will be discussed in detail and the similaries and differences between the tests will be compared and discussed. The first three tests were used to analyze what the APEX facility could produce in terms of condensation rates and inlet steam Reynolds Numbers through Steam Generator #1. Following the data analysis for the first three tests, three more tests were developed in order to increase the inlet steam Reynolds Number to the facility maximum.

The Six Test Overview

Table 4.1 – Overview of the Six NRC Condensation Tests

Test Number	Description
NRC-COND-01	SG condensation with various steam inlet/outlet flow rates. • Steam pressure: 1.48 MPa (215 psia). • Inlet gas Re=2000—5300.
NRC-COND-02	SG condensation with various steam inlet/outlet flow rates. • Steam pressure: 2.03 MPa (295 psia). • Inlet gas 2100—4700.
NRC-COND-03	SG condensation with various steam inlet/outlet flow rates. • Steam pressure: 0.793 MPa (115 psia). • Inlet gas Re=7700—12600.
NRC-COND-04	SG condensation with various steam inlet/outlet flow rates. • Steam inlet pressure: 2.17 MPa (315 psia). • Inlet gas Re=7700—12700.
NRC-COND-05	SG condensation with various steam inlet/outlet flow rates. • Steam inlet pressure: 2.38 MPa (345 psia). • Inlet gas Re=8000—12400.
NRC-COND-06	SG condensation with various steam inlet/outlet flow rates. • Steam inlet pressure: 0.45 MPa (65 psia). • Inlet gas Re=3200—8000.

Table 4.1 shows the test matrix completed for the NRC Condensation tests performed between 2005 and 2007. Important information is the nominal pressure for the system and the range of Reynolds Number. Condensation rates and other information will be discussed for each individual test.

NRC-Condensation-001

The first condensation test was performed at a facility pressure of 1.482 MPa (215 psia). This test had five steps associated with it. Table 4.2 shows the nominal test conditions for all of the steps during this test. Figure 4.1 shows the normalized catch tank level for each of the five steps of NRC-Condensation-001. Figure 4.2 shows the normalized separator level for each of the five steps of NRC-Condensation-001. Each of the figures are normalized to show the change in level for the duration of the ten minute (600 second) test.

Table 4.2 – Nominal Test Conditions for NRC-Condensation-001

Step	SG #1 Pressure - Mpa (psia)	SG#1 Inlet Energy - kW	SG#1 Outlet Energy - kW	SG#1 Shell Side Energy - kW
1	1.482 ± .0072 (215.0 ± 1.038)	0	0	0
2	1.482 ± .0072 (215.0 ± 1.038)	377.04 ± 4.29	273.41 ± 3.13	91.29 ± 1.05
3	1.482 ± .0072 (215.0 ± 1.038)	330.98 ± 3.73	216.36 ± 2.45	96.97 ± 1.11
4	1.482 ± .0072 (215.0 ± 1.038)	232.99 ± 2.59	104.47 ± 1.16	104.95 ± 1.18
5	1.482 ± .0072 (215.0 ± 1.038)	135.79 ± 1.5	0	111.06 ± 1.23

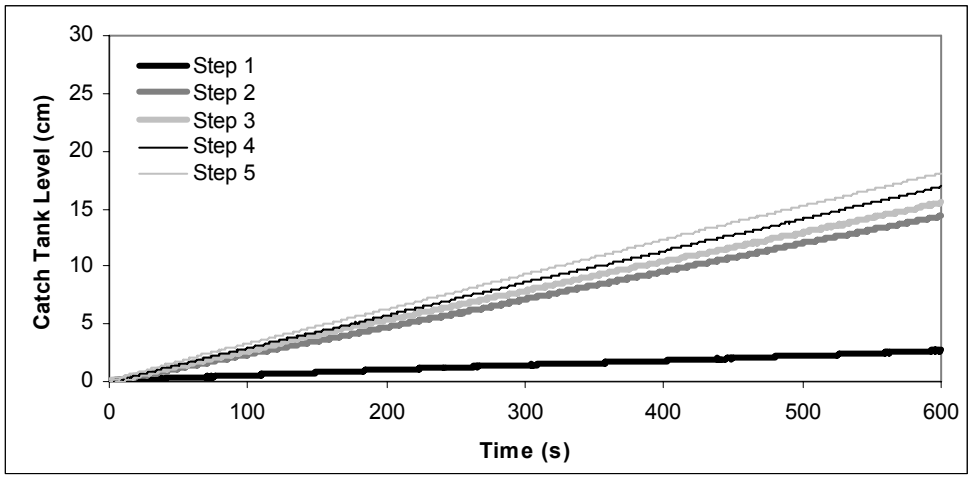

Figure 4.1 – Catch Tank Level for NRC-Condensation-001

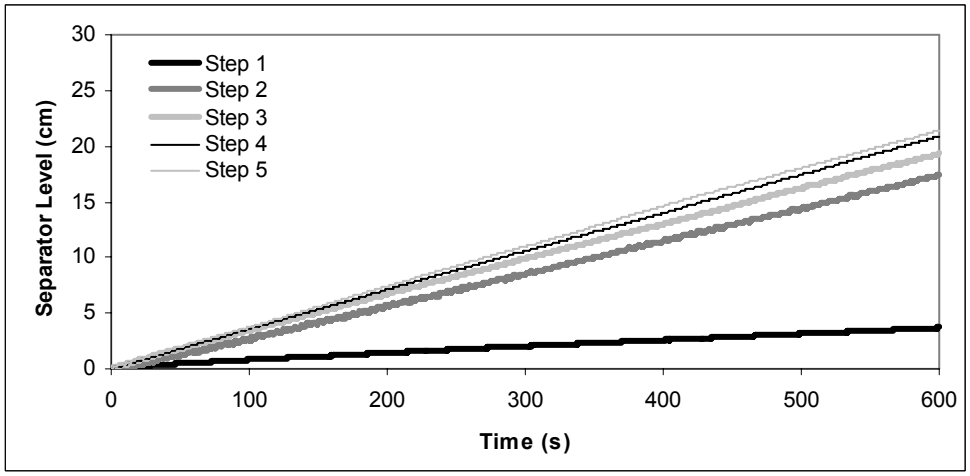

Figure 4.2 – Separator Level for NRC-Condensation-001

NRC-Condensation-002

The second condensation test was performed at a facility pressure of 2.03 MPa (295 psia). This test had five steps associated with it. Table 4.3 shows the nominal test conditions for all of the steps during this test. Figure 4.3 shows the

normalized catch tank level for each of the five steps of NRC-Condensation-002. Figure 4.4 shows the normalized separator level for each of the five steps of NRC-Condensation-002. Each of the figures are normalized to show the change in level for the duration of the ten minute (600 second) test.

Table 4.3 – Nominal Test Conditions for NRC-Condensation-002

Step	SG #1 Pressure - Mpa (psia)	SG#1 Inlet Energy - kW	SG#1 Outlet Energy - kW	SG#1 Shell Side Energy - kW
1	2.034 ± .0072 (295.0 ± 1.038)	0	0	0
2	2.034 ± .0072 (295.0 ± 1.038)	427.42 ± 4.61	286.44 ± 3.09	116.28 ± 1.26
3	2.034 ± .0072 (295.0 ± 1.038)	349.87 ± 3.75	197.85 ± 2.12	123.71 ± 1.33
4	2.034 ± .0072 (295.0 ± 1.038)	284.81 ± 3.04	120.44 ± 1.29	128.81 ± 1.38
5	2.034 ± .0072 (295.0 ± 1.038)	168.54 ± 1.79	0	136.02 ± 1.45

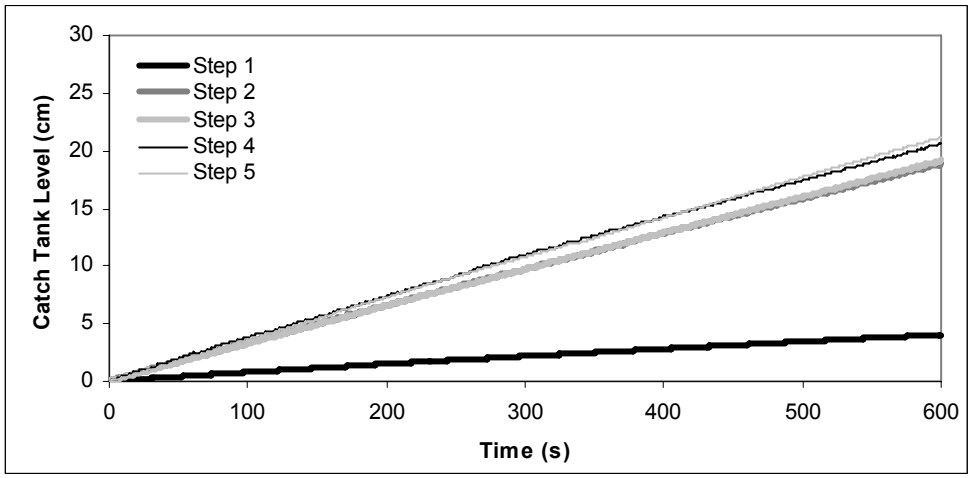

Figure 4.3 – Catch Tank Level for NRC-Condensation-002

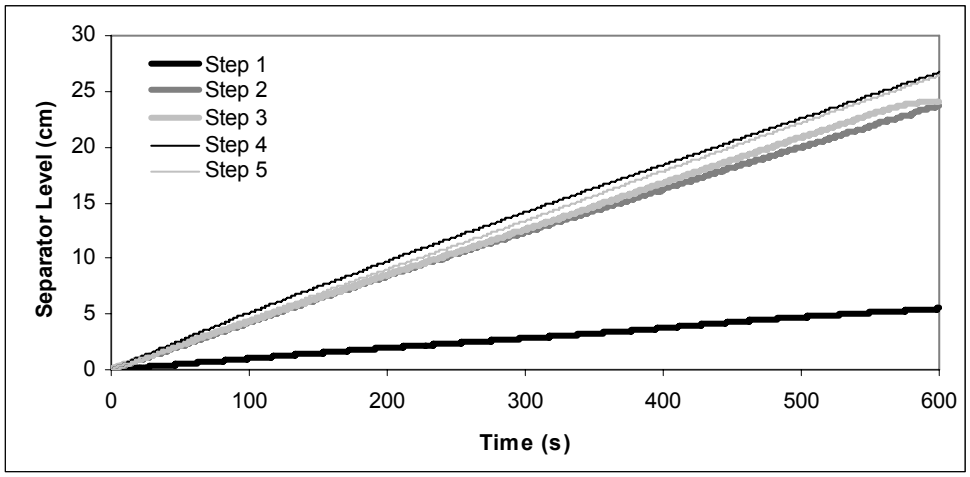

Figure 4.4 – Separator Level for NRC-Condensation-002

NRC-Condensation-003

The third condensation test was performed at a facility pressure of 0.793 MPa (115 psia). This test had five steps associated with it. Table 4.4 shows the nominal test conditions for all of the steps during this test. Figure 4.5 shows the normalized catch tank level for each of the five steps of NRC-Condensation-003. Figure 4.6 shows the normalized separator level for each of the five steps of NRC-Condensation-003. Each of the figures are normalized to show the change in level for the duration of the ten minute (600 second) test.

Table 4.4 – Nominal Test Conditions for NRC-Condensation-003

Step	SG #1 Pressure - Mpa (psia)	SG#1 Inlet Energy - kW	SG#1 Outlet Energy - kW	SG#1 Shell Side Energy - kW
1	0.793 ± .0072 (115.0 ± 1.038)	0	0	0
2	0.793 ± .0072 (115.0 ± 1.038)	311.15 ± 4.91	218.52 ± 3.7	83.43 ± 1.47
3	0.793 ± .0072 (115.0 ± 1.038)	283.94 ± 4.26	158.97 ± 2.48	94.99 ± 1.56
4	0.793 ± .0072 (115.0 ± 1.038)	248.79 ± 3.58	114.46 ± 1.68	105.06 ± 1.63
5	0.793 ± .0072 (115.0 ± 1.038)	136.57 ± 1.82	0	100.31 ± 1.39

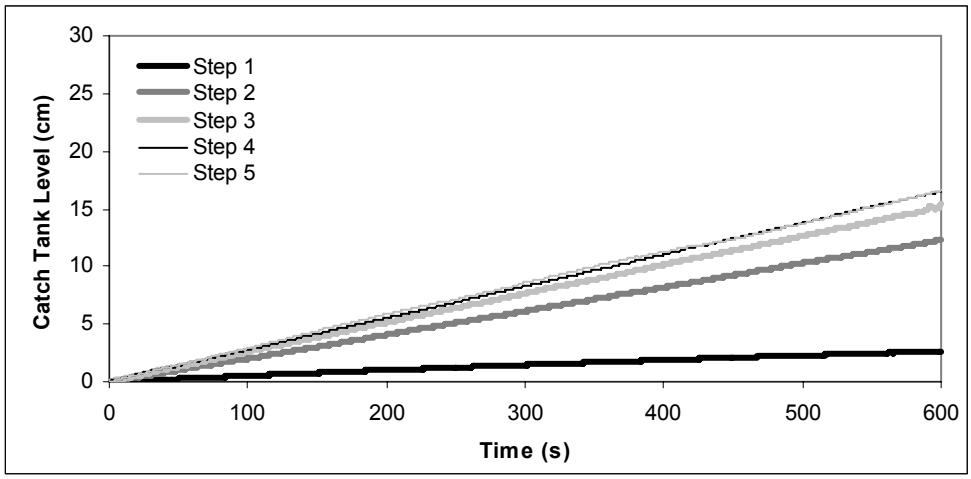

Figure 4.5 – Catch Tank Level for NRC-Condensation-003

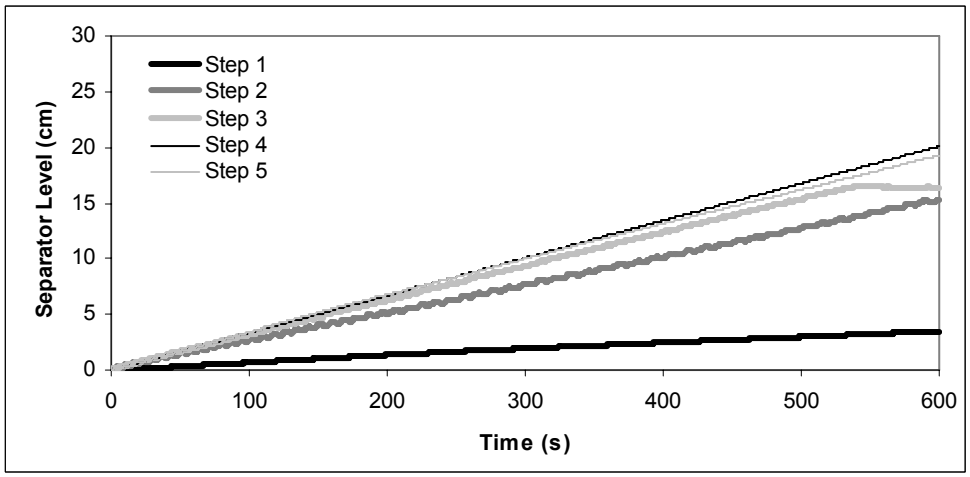

Figure 4.6 – Separator Level for NRC-Condensation-003

NRC-Condensation-004

The fourth condensation test was performed at a facility pressure of 2.17 MPa (315 psia). This test had four steps associated with it. Table 4.5 shows the nominal test conditions for all of the steps during this test. Figure 4.7 shows the normalized catch tank level for each of the four steps of NRC-Condensation-004.

Figure 4.8 shows the normalized separator level for each of the four steps of NRC-Condensation-004. Each of the figures are normalized to show the change in level for the duration of the ten minute (600 second) test.

Table 4.5 – Nominal Test Conditions for NRC-Condensation-004

Step	SG #1 Pressure - Mpa (psia)	SG#1 Inlet Energy - kW	SG#1 Outlet Energy - kW	SG#1 Shell Side Energy - kW
1	2.17 ± .0072 (315.0 ± 1.038)	0	0	0
2	2.17 ± .0072 (315.0 ± 1.038)	552.96 ± 5.87	375.99 ± 3.99	140.2 ± 1.5
3	2.17 ± .0072 (315.0 ± 1.038)	696.2 ± 7.42	523.22 ± 5.58	135.76 ± 1.45
4	2.17 ± .0072 (315.0 ± 1.038)	914.3 ± 9.79	739.06 ± 7.92	130.24 ± 1.4

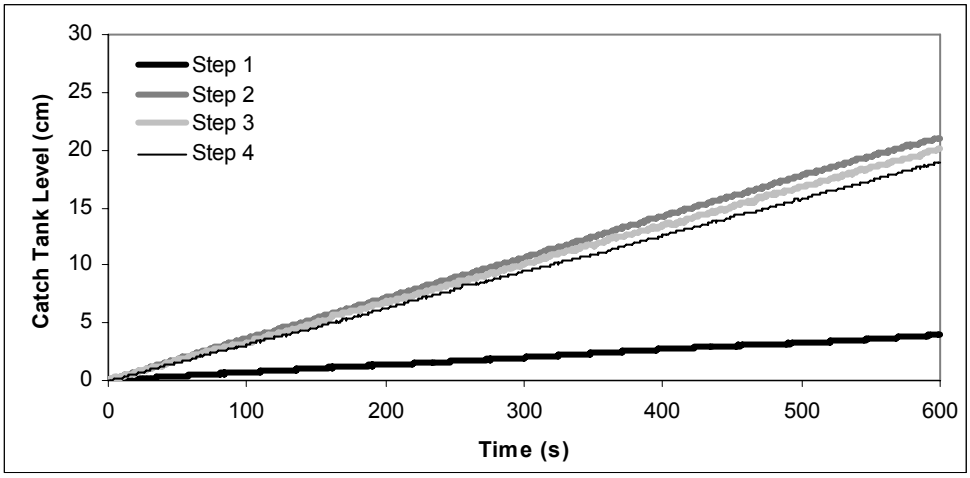

Figure 4.7 – Catch Tank Level for NRC-Condensation-004

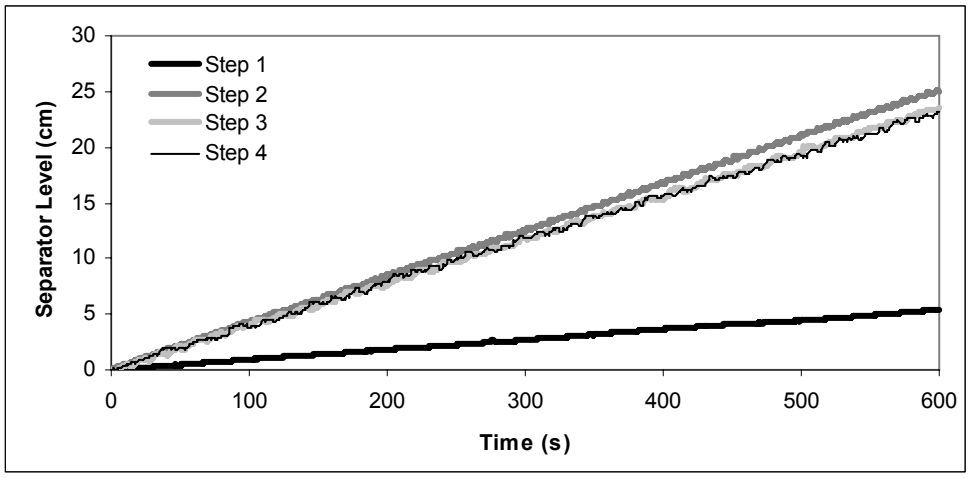

Figure 4.8 – Separator Level for NRC-Condensation-004

NRC-Condensation-005

The fifth condensation test was performed at a facility pressure of 2.38 MPa (345 psia). This test had four steps associated with it. Table 4.6 shows the nominal test conditions for all of the steps during this test. Figure 4.9 shows the normalized catch tank level for each of the four steps of NRC-Condensation-005. Figure 4.10 shows the normalized separator level for each of the four steps of NRC-Condensation-005. Each of the figures are normalized to show the change in level for the duration of the ten minute (600 second) test.

Table 4.6 – Nominal Test Conditions for NRC-Condensation-005

Step	SG #1 Pressure - Mpa (psia)	SG#1 Inlet Energy - kW	SG#1 Outlet Energy - kW	SG#1 Shell Side Energy - kW
1	2.38 ± .0072 (345.0 ± 1.038)	0	0	0
2	2.38 ± .0072 (345.0 ± 1.038)	587.06 ± 6.17	396.96 ± 4.17	160.94 ± 1.7
3	2.38 ± .0072 (345.0 ± 1.038)	703.42 ± 7.41	517.06 ± 5.45	156.07 ± 1.65
4	2.38 ± .0072 (345.0 ± 1.038)	909.02 ± 9.61	722.98 ± 7.64	150.33 ± 1.6

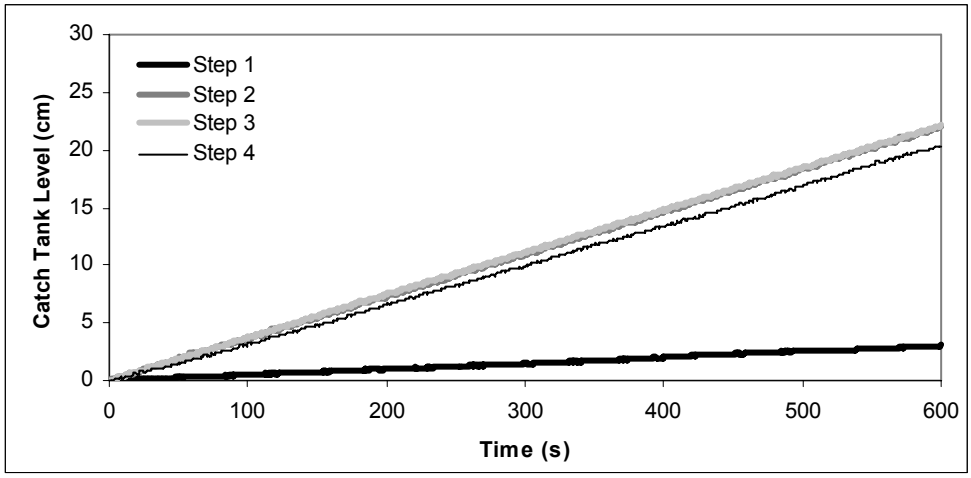

Figure 4.9 – Catch Tank Level for NRC-Condensation-005

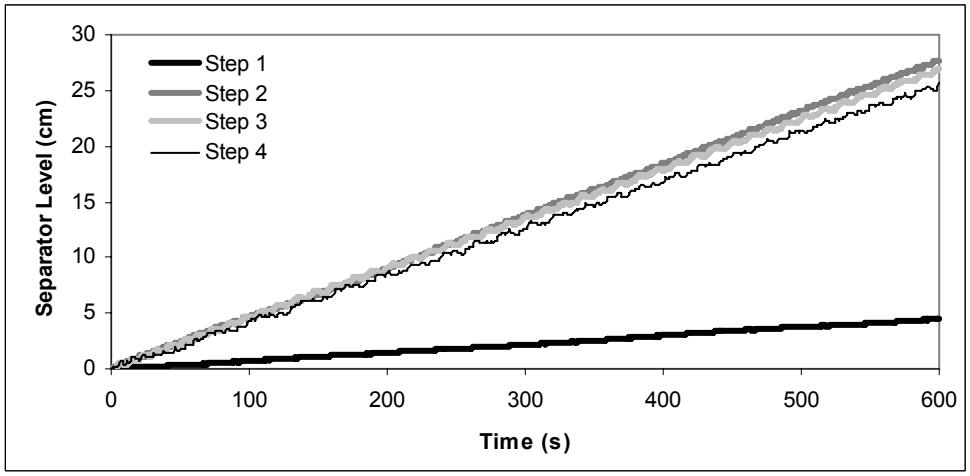

Figure 4.10 – Separator Level for NRC-Condensation-005

NRC-Condensation-006

The sixth condensation test was performed at a facility pressure of 0.45 MPa (65 psia). This test had five steps associated with it. Table 4.7 shows the nominal test conditions for all of the steps during this test. Figure 4.11 shows the

normalized catch tank level for each of the five steps of NRC-Condensation-006. Figure 4.12 shows the normalized separator level for each of the five steps of NRC-Condensation-006. Each of the figures are normalized to show the change in level for the duration of the ten minute (600 second) test.

Table 4.7 – Nominal Test Conditions for NRC-Condensation-006

Step	SG #1 Pressure - Mpa (psia)	SG#1 Inlet Energy - kW	SG#1 Outlet Energy - kW	SG#1 Shell Side Energy - kW
1	0.450 ± .0072 (65.0 ± 1.038)	0	0	0
2	0.450 ± .0072 (65.0 ± 1.038)	192.99 ± 3.54	102.84 ± 1.89	81.52 ± 1.65
3	0.450 ± .0072 (65.0 ± 1.038)	279.88 ± 5.25	193.18 ± 3.68	78.36 ± 1.63
4	0.450 ± .0072 (65.0 ± 1.038)	376.7 ± 7.3	283.61 ± 5.68	83.14 ± 1.84
5	0.450 ± .0072 (65.0 ± 1.038)	513.21 ± 10.59	358.45 ± 8.22	80.21 ± 1.98

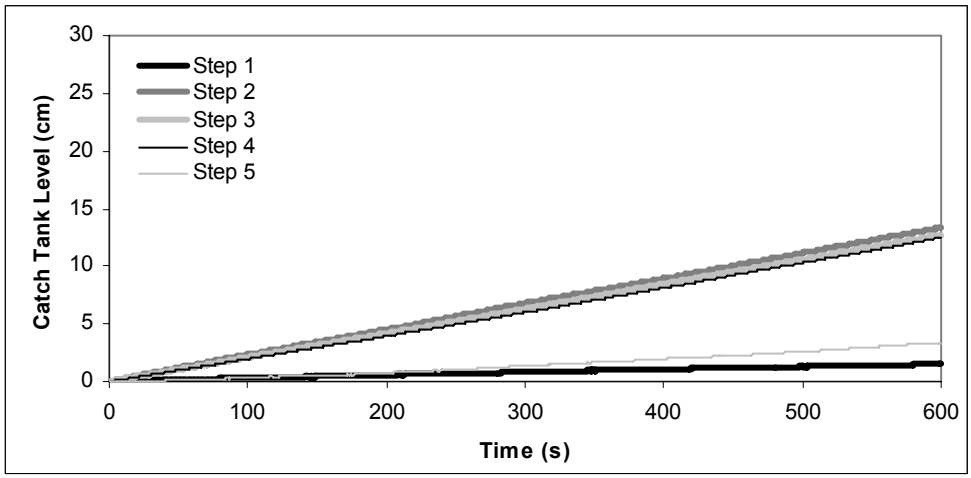

Figure 4.11 – Catch Tank Level for NRC-Condensation-006

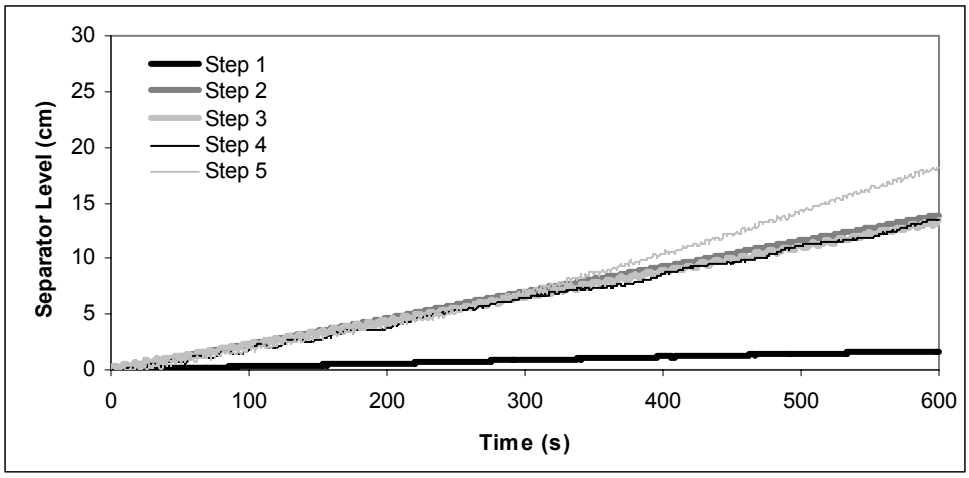

Figure 4.12 – Separator Level for NRC-Condensation-006

ANALYSIS

From the figures above, it is shown that the condensation rates during the tests are constant. The only case where that is not true is Step 5 of NRC-Condensation-006. Table 4.8 shows the average condensation rates, steam flow rates, and velocities for each step and test. The isentropic expansion through the valve into the catch tank is considered in the hot leg condensation rates.

Table 4.8 – Average Condensation and Volumetric Flow Rates

Test NRC-Condensation-01	Step 2	Step 3	Step 4	Step 5
Steam inlet flow (kg/hr)	487.23	427.49	300.70	175.15
U-tube steam inlet velocity (m/s)	0.84	0.71	0.47	0.26
Steam outlet flow (kg/hr)	353.42	279.49	134.84	0.35
U-tube steam outlet velocity (m/s)	0.63	0.47	0.21	0.00
HL U-tube condensation rate (kg /hr)	69.83	75.93	83.31	89.30
CL U-tube condensation rate (kg /hr)	66.23	73.15	78.70	80.30
Test NRC-Condensation-02	**Step 2**	**Step 3**	**Step 4**	**Step 5**
Steam inlet flow (kg /hr)	550.47	450.41	366.55	216.84
U-tube steam inlet velocity (m/s)	0.70	0.55	0.43	0.24
Steam outlet flow (kg /hr)	368.97	254.72	155.01	0.47
U-tube steam outlet velocity (m/s)	0.48	0.31	0.18	0.00
HL U-tube condensation rate (kg /hr)	94.01	96.05	103.99	106.95
CL U-tube condensation rate (kg /hr)	88.36	88.97	98.67	97.49
Test NRC-Condensation-03	**Step 2**	**Step 3**	**Step 4**	**Step 5**
Steam inlet flow (kg /hr)	406.93	370.82	324.51	177.69
U-tube steam inlet velocity (m/s)	1.55	1.30	1.06	0.50
Steam outlet flow (kg /hr)	286.32	207.83	149.39	0.11
U-tube steam outlet velocity (m/s)	1.22	0.78	0.50	0.00
HL U-tube condensation rate (kg /hr)	56.03	70.93	76.34	77.93
CL U-tube condensation rate (kg /hr)	60.86	64.26	78.86	75.10
Test NRC-Condensation-04	**Step 2**	**Step 3**	**Step 4**	
Steam inlet flow (kg /hr)	711.45	895.94	1177.03	
U-tube steam inlet velocity (m/s)	0.81	1.04	1.43	
Steam outlet flow (kg /hr)	483.75	673.35	951.51	
U-tube steam outlet velocity (m/s)	0.55	0.79	1.17	
HL U-tube condensation rate (kg /hr)	106.27	101.18	94.95	
CL U-tube condensation rate (kg /hr)	92.29	87.20	86.01	
Test NRC-Condensation-05	**Step 2**	**Step 3**	**Step 4**	
Steam inlet flow (kg /hr)	754.77	904.48	1169.12	
U-tube steam inlet velocity (m/s)	0.77	0.94	1.26	
Steam outlet flow (kg /hr)	510.35	664.86	929.89	
U-tube steam outlet velocity (m/s)	0.52	0.69	1.01	
HL U-tube condensation rate (kg /hr)	112.41	112.72	103.05	
CL U-tube condensation rate (kg /hr)	101.09	98.74	94.15	
Test NRC-Condensation-06	**Step 2**	**Step 3**	**Step 4**	**Step 5**
Steam inlet flow (kg /hr)	253.35	367.62	495.16	675.54
U-tube steam inlet velocity (m/s)	1.20	1.80	2.53	3.73
Steam outlet flow (kg /hr)	135.01	253.83	373.07	472.90
U-tube steam outlet velocity (m/s)	0.64	1.27	1.99	2.97
HL U-tube condensation rate (kg /hr)	60.48	57.24	56.19	14.93
CL U-tube condensation rate (kg /hr)	55.28	53.65	54.20	72.94

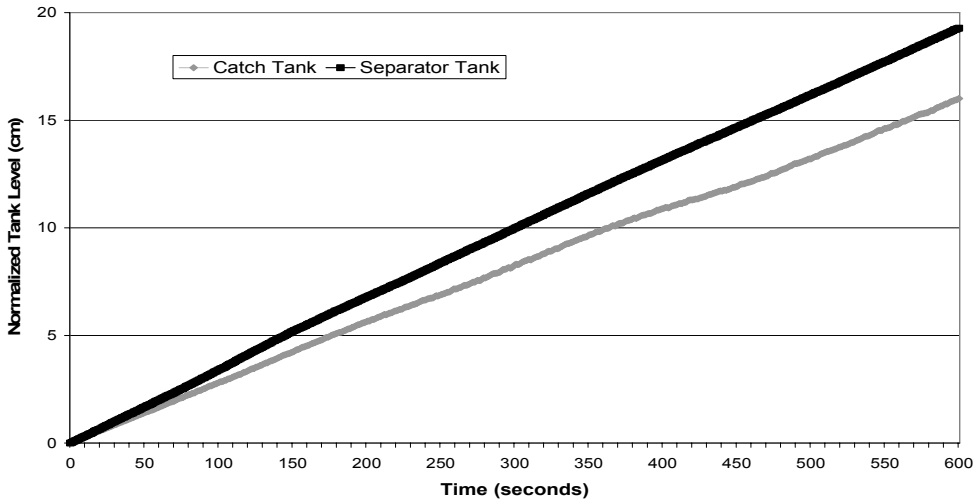

Figure 4.13 – Normalized Tank Levels for NRC-Condensation-004 Step 5

Analyzing the data from a particular step and test, it is shown that the collapsed liquid level for the catch tank and separator tank are different. Figure 4.13 shows that the separator tank (cold leg) records a higher condensation rate than the catch tank (hot leg). This is due to the collapsed liquid level of the catch tank under predicting the condensation rates for the hot leg. As the condensate leaves the pressurized system, some of it flashes to steam and is not measured as liquid water. For the mass balance, this steam is measured with flow meter FVM-004 for all of the tests.. When the expansion and flashing is taken into account, the condensation rates for both the hot leg and cold legs are very similar. The only exception is Test-6 Step-5 where the steam inlet velocity was at its highest.

Chapter 5 – Discussion

Non-Dimensional Number Analysis

Since many different experiments have been completed involving condensation and each one of them is different, non-dimensional numbers are used to compare the results from different tests. Works previously completed involving condensation have focused on three main non-dimensional numbers which include the Reynolds number, the Nusselt number, and the Prandtl number. These non-dimensional numbers can be used for steam flow and condensate flow both turbulent and laminar and are usually important in the analysis of heat transfer in fluids. Other non-dimensional numbers have been used in heat transfer analysis for both flat plates and tubes include the Froude number, Grashoff number, Jakob number, and the Galileo number. Some of these numbers are only important and only apply to certain flow regimes or geometries and can be ignored for certain cases.

In order to determine which non-dimensional numbers are of importance for this particular experiment, a Buckingham Pi analysis was done. Table 5.1 shows the variables of interest and their corresponding mass, length, time, and temperature terms. Having eleven variables and four dimensions implies that for this Buckingham Pi analysis, seven Pi groups may exist.

After choosing the repeating variables and performing the analysis, dimensionless groups fall out of the equations. The non-dimensional number potentially important to this analysis can be seen in the equations below.

Table 5.1 – Variables for Buckingham Pi analysis

Property	Dimensions
ρ - fluid and gas	$M L^{-3}$
μ - fluid and gas	$M L^{-1} T^{-1}$
V - gas velocity	$L T^{-1}$
d - tube diameter	L
g - gravitational	$L T^{-2}$
k_f - thermal conductivity of fluid	$M L T^{-3} \theta^{-1}$
c_p - specific heat	$L^2 T^{-2} \theta^{-1}$
T_{sat} - saturation temp.	θ
T_∞ - Bulk Fluid Temp	θ
h - heat transfer coefficient	$M T^{-3} \theta^{-1}$
m_{dot} – condensate mass flow rate	$M T^{-3}$

Since this is a fluids problem and the viscous forces do not dominate the system, the Reynolds number is of importance. Comparing the Reynolds number to the Nusselt number determines the flow regime that the steam or condensate film is in. The flow regime determines the amount of heat transferred to and from the steam and condensate. As the film Reynolds number increases in the laminar regime the film thickness increases and the heat transfer decreases, however, when the film is in the turbulent regime, the film thickness still increases with increasing film Reynolds number but the heat transfer also increases. In these experiments the Reynolds number for the steam inlet flow (Equation 5.1) and for the film condensate flow (Equation 5.2) are calculated.

$$\mathrm{Re}_{steam} = \frac{\rho_g V_g d}{\mu_g} \tag{5.1}$$

$$\mathrm{Re}_{film} = \frac{4\Gamma}{\mu_f} \qquad \text{Where} \qquad \Gamma = \frac{\dot{m}_{condensate}}{\pi d} \tag{5.2}$$

Where ρ_f and ρ_g is the density of the fluid and gas respectively, μ_f and μ_g is the viscosity of the fluid and gas respectively, d is the diameter, V is the steam

velocity, g is the gravitational constant, Γ is the condensate mass flow rate per unit length, and δ is the characteristic length for the condensate film thickness.

The Nusselt number is used to compare the heat transfer characteristics for a particular flow regime. It takes into account that conduction heat transfer and convective heat transfer occur together. The overall heat transfer is higher when compared to just conduction heat transfer, so using the Nusselt number gives a better representation of what is actually occurring. In its original form, it can be seen in Equation 5.3, where L is the characteristic length which is d for a tube. The Nusselt number modified for condensation can be seen in Equation 5.4. The characteristic length term, L, from the original form is replaced with a condensation characteristic length. This characteristic length can be seen in Equation 5.4 as the cube root term. The density, viscosity, and gravitational forces are considered for the condensate film.

$$Nu = \frac{hL}{k_f} \tag{5.3}$$

$$Nu_{\text{mod}} = \frac{\bar{h}}{k_f}\left[\frac{\mu_f^2}{\rho_f\left(\rho_f - \rho_g\right)g}\right]^{\frac{1}{3}} \tag{5.4}$$

Where h is the heat transfer coefficient, k_f is the thermal conductivity of the film.

Convection for heat transfer plays a role in these experiments. In order to determine how effective the convection heat transfer is compared to conduction heat transfer, the Prandtl number is introduced. The Prandtl number represents the ratio of momentum diffusivity to thermal diffusivity. Small values represent conduction as the dominate heat transfer method, while large values show that

convection is the dominate method. The Prandtl number formula can be seen in Equation 5.5.

$$\mathrm{Pr} = \frac{c_{p,f}\,\mu_f}{k_f} \tag{5.5}$$

Where $c_{p,f}$ is the specific heat at constant pressure for the fluid.

The Buckingham Pi method gives non dimensional numbers that may or may not be of some importance. For the remaining non-dimensional numbers, the Froude number (Equation 5.6) is used for free surface flows and has little importance for these experiments since objects are not moving though the fluids, the Grashoff number (Equation 5.7) is used to describe natural convection and can be combined with the Prandtl number to give the Raleigh number. The Jakob number (Equation 5.8) is the ratio of heat required to reach saturation temperature over the latent heat of vaporization which could be important when heating subcooled liquids, and the Galileo number (Equation 5.9) which compares gravitational forces to viscous forces and may be of use with the film condensation flow inside the U-tubes.

$$Fr = \frac{U^2}{gd} \tag{5.6}$$

$$Gr = \frac{\beta \cdot \Delta T \cdot g \cdot d^3 \rho^2}{\mu^2} \tag{5.7}$$

$$Ja = \frac{\rho_f c_{p,f} \Delta T}{\rho_g \cdot h_{fg}} \tag{5.8}$$

$$Ga = \frac{gd^3}{\upsilon^2} \tag{5.9}$$

With these numbers it is possible to compare these experiments to other experiments or calculations where the geometry or phenomena observed may or may not be the same.

The comparison of the above numbers for all of the tests will give us an indication as to what is happening inside the U-tubes. Since these same non-dimensional numbers were also used in other experiments, these results can compared with other experiments.

Heat Transfer

Since the only instrumentation inside the U-tube bundle are six thermocouples, the overall heat transfer coefficient has to be calculated from instrument data on the inside and outside of the tubes. The first step is to determine the overall heat transfer coefficient from the tube inside to the steam generator secondary side. From the volumetric flow meter and pressure transducer on the secondary side, the amount of steam leaving the system is measured and a corresponding energy out can be calculated. Assuming saturated liquid on the steam generator secondary side and using the average temperature inside the U-tubes from the thermocouples to determine the temperature difference, along with the tube bundle outside surface area, Equation 5.10 can be used to solve for the overall heat transfer coefficient.

$$E_{out} = U \cdot A \cdot \Delta T \Rightarrow U = \frac{E_{out}}{A \cdot \Delta T} \tag{5.10}$$

The heat transfer coefficient through the condensate layer is of importance, however with limited instrumentation inside the tubes, the only way to determine the coefficient is to back calculate it from the overall heat transfer coefficient.

Using an equivalent thermal circuit, the condensate heat transfer coefficient can be determined. Equation 5.11 shows the equation for the thermal circuit with R_1, R_2, and R_3 being the resistances encountered through the tube. R_1 is the resistance through the condensate layer, R_2 is the resistance through the tube wall, and R_3 is the resistance of boiling on the outside of the U-tube walls.

$$\frac{1}{U} = \frac{1}{R_1} + \frac{1}{R_2} + \frac{1}{R_3} \tag{5.11}$$

Putting the variables for convective heat transfer and conductive heat transfer through the U-tube geometry into Equation 5.11 and rearranging to calculate the overall heat transfer coefficient gives Equation 5.12.

$$U = \frac{1}{\frac{1}{h_i} + \frac{r_i}{k_w}\ln\left(\frac{r_o}{r_i}\right) + \frac{r_i}{r_o h_o}} \tag{5.12}$$

Equation 5.12 uses the inside and outside tube radius with the thermal conductivity of the stainless steel tube. The only other piece of the equation that is needed is the heat transfer coefficient for boiling on the outside of the tube (h_o). This can be calculated as saturated nucleate pool boiling using the Cooper method and can be seen in Equations 5.13 and 5.14 (Cooper 1960).

$$h_o = 55P_r^n\left(-0.4343\ln\left(P_r\right)\right)^{-0.55}M^{-0.5}\left(q''\right)^{0.67} \quad (5.13)$$

$$n = 0.12 - 0.4343\ln\left(R_p\right) \quad (5.14)$$

Where P_r is the reduced pressure, M is the molecular weight, and q" is the heat flux on the tube exterior. Using all of the known information with Equations 5.12 – 5.14, the condensate heat transfer coefficient can be calculated for each test and step.

Modified Nusselt Number

Due to error propagation and limited instrumentation inside the U-tube bundle, the error in calculating the modified Nusselt number ranges from 40% to 51%. The figures below show the relationship between the modified Nusselt number and the other important non-dimensional quantities.

Figure 5.1 shows the relationship between the modified Nusselt number and the condensate film Reynolds number.

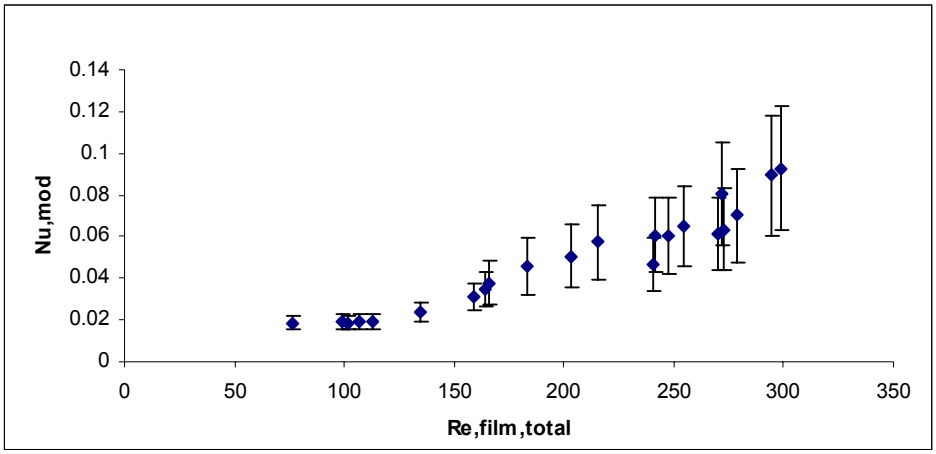

Figure 5.1 – Modified Nusselt Number versus Total Film Reynolds Number

With the film Reynolds number range between roughly 50 and 300 and comparing it to the flat plate analysis, it would be expected that the flow regime would be laminar-wavy. However, with an increasing modified Nusselt number as a function of the film Reynolds number, the regime resembles turbulent flow for a film Reynolds number greater than 125. For film Reynolds number less than 125, the Nusselt number remains relatively constant which represents the laminar-wavy regime.

The comparison between the modified Nusselt numbers and the inlet steam Reynolds numbers, shown in Figure 5.2, does not give any correlation, and it suggests that the modified Nusselt number is not a direct function of the steam inlet Reynolds number.

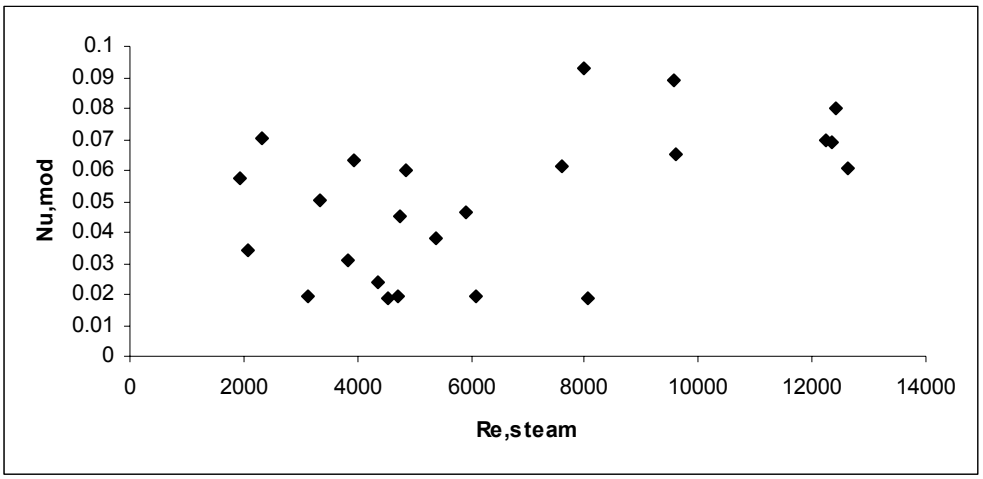

Figure 5.2 – Modified Nusselt Number versus Steam Inlet Reynolds Number

With a relationship between the modified Nusselt number and both the film Reynolds and film Prandtl numbers, the relation between the three of values could

potentially be interesting. Figure 5.3 shows the relationship between the film Reynolds number, the modified Nusselt number, and the film Prandtl number. As the Prandtl number increases, the modified Nusselt number should increase, however the data does not show that trend. Reasons for this may include the small range of Prandtl number compared to the large range of Reynolds number. Using the flat plate equations, Figure 5.4 shows the expected change in the modified Nusselt number as both the film Reynolds number and Prandtl number increases.

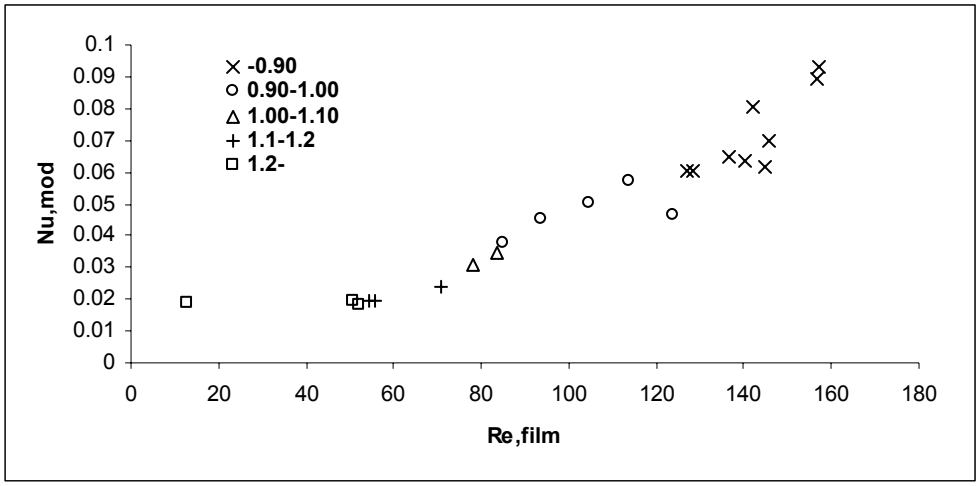

Figure 5.3 – Modified Nu Number vs Film Re with Film Pr

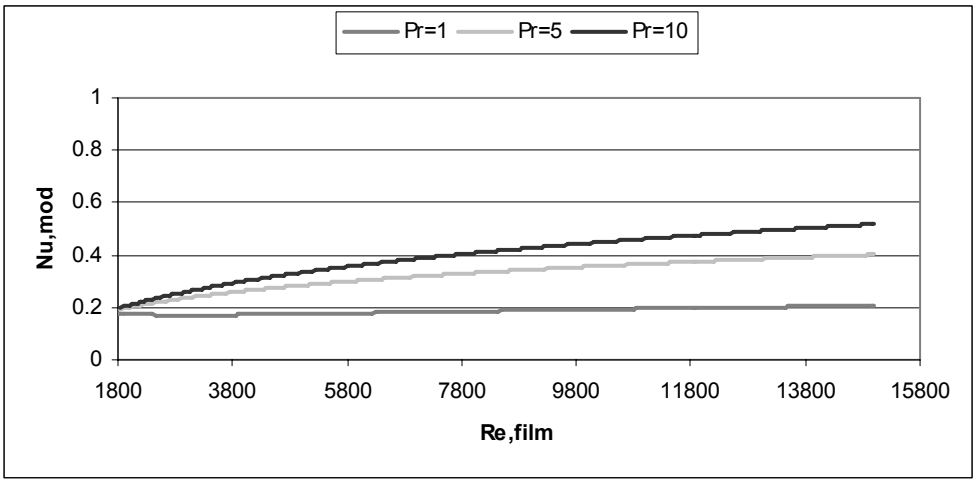

Figure 5.4 – Modified Nusselt Number as Prandtl Number Increases

The APEX data in Figure 5.3 shows that as the film Prandtl number decreases, both the modified Nusselt number and film Reynolds number increase as well. The reason for this is the inverse correlation between the Reynolds number and Prandtl number in the APEX tests. Figure 5.5 shows the relationship between the film Prandtl number and the film Reynolds number.

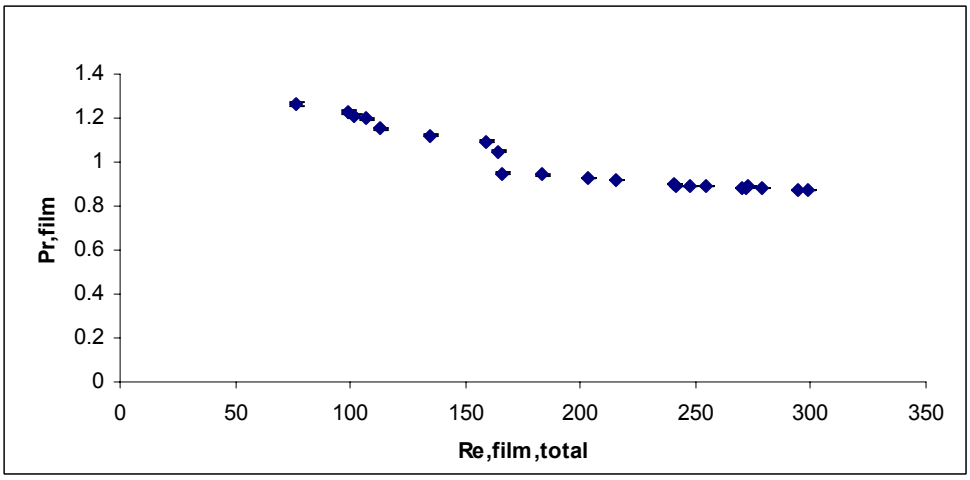

Figure 5.5 – Film Prandtl Number versus Film Reynolds Number

It shows that as the film Prandtl number decreases, the film Reynolds number increases. The range of Prandtl numbers (0.9-1.2) is not sufficient to determine the effectiveness of Prandtl number on heat transfer for these experiments.

Condensate Carryover

During these experiments, the condensation rate on both the hot and cold legs was roughly the same except for one case. It is believed that on this one case the tube velocities were high enough to push the condensate onto the cold leg side. Figure 5.6 shows the normalized separator and catch tank levels for Test 6 Step 5.

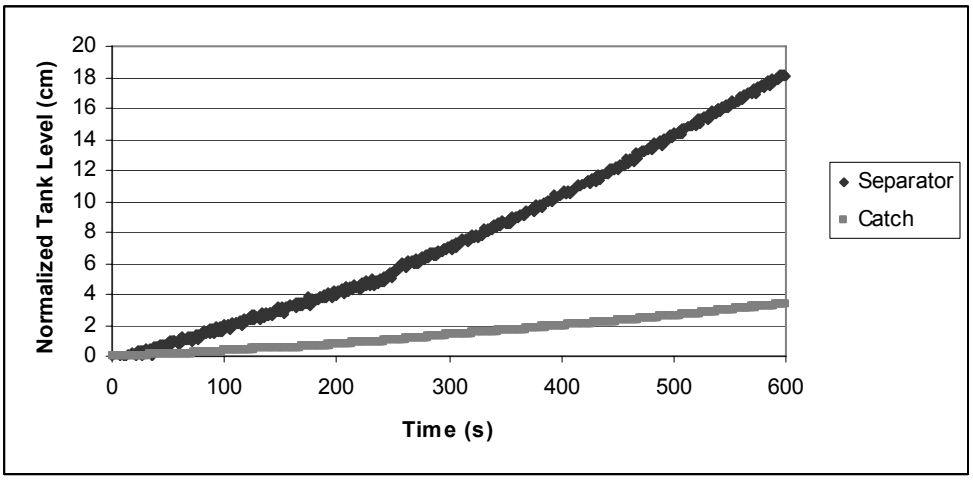

Figure 5.6 – Normalized Separator and Catch Tank Levels – Test 6 Step 5

The figure shows that the more condensate collected in the separator tank than in the catch tank. From Table 4.8 it was shown that the steam inlet velocity was 3.73 meters per second. Since this was the only step where there was a noticeable condensation carryover, the exact vapor velocity required for condensate carryover for the experimental setup was undetermined. This was also the test and step

where the mass and energy balances had the greatest error. Conclusions involving this step cannot be made without further examination. Equation 5.15 shows the condensate carryover ratio. This gives the relative difference between the hot and cold leg condensation rates.

$$C = \frac{\mathrm{Re}_{film,cold}}{\mathrm{Re}_{film,hot}} \tag{5.15}$$

For most of the tests the carry-over ratio is very close to one. The following figures show the relationship between the condensate carryover with the steam inlet Reynolds number (Figure 5.7), the film Reynolds number (Figure 5.8), and the modified Nusselt number (Figure 5.9).

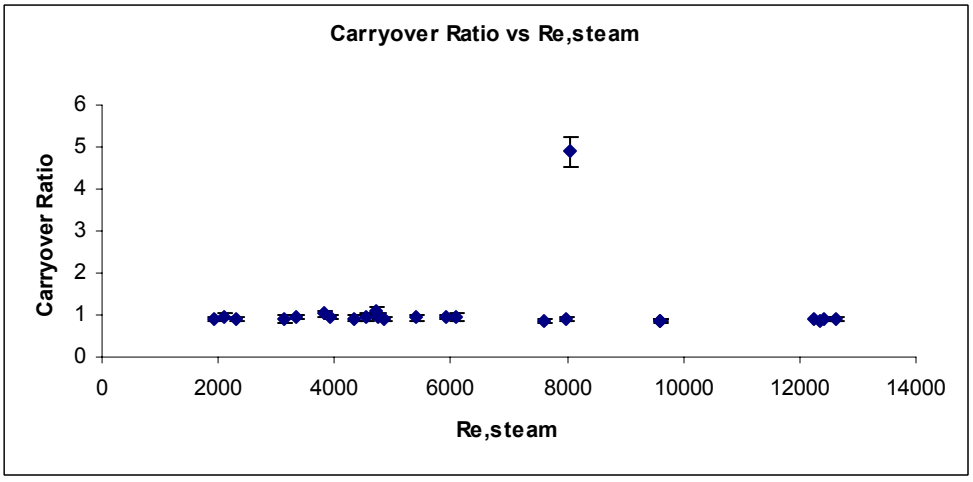

Figure 5.7 – Carryover Ratio versus Steam Inlet Reynolds Number

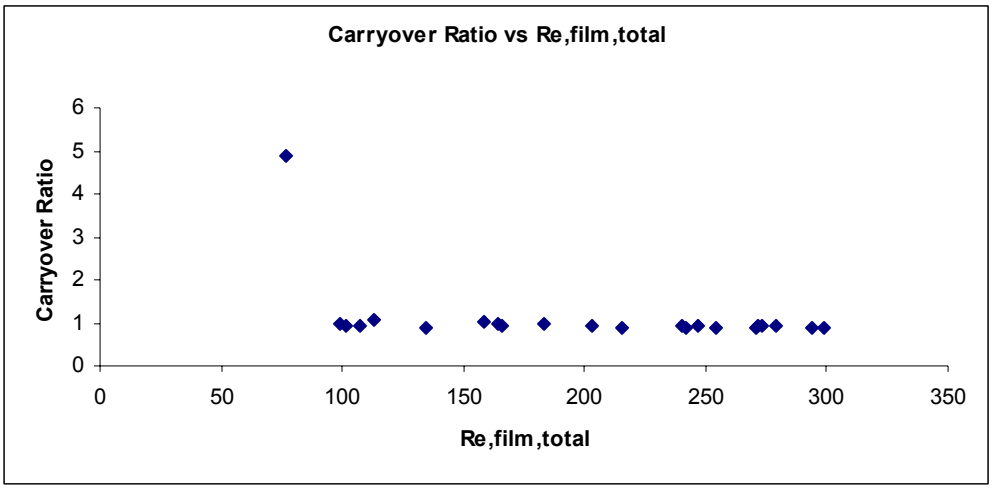

Figure 5.8 – Carryover Ratio versus Film Reynolds Number

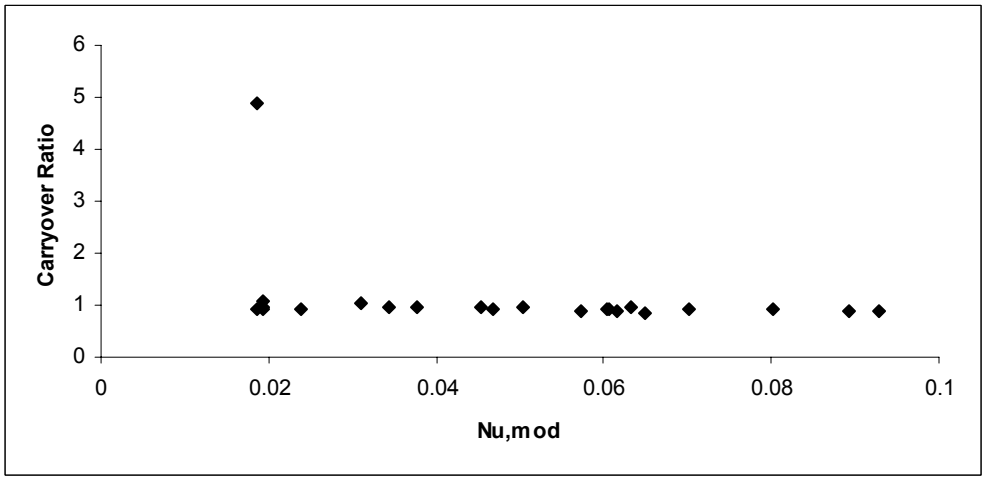

Figure 5.9 – Carryover Ratio versus Modified Nusselt Number

Again, since there is only one data point that is greater than one, it is impossible to determine if there is a relationship between the carryover ratio and any of the non-dimensional numbers. The only conclusion that can be made is that there seems to be no relationship between the steam inlet Reynolds number and the carryover ratio. All of the other relationships need more data where the carryover ratio is greater than one to determine if there is a relationship.

Interfacial Shear Stress

As discussed in Chapter 2, the interfacial shear stress should be considered in experiments where there is a gas-liquid interface. In these experiments, the interfacial shear stress may affect the regime for the condensate film pushing it into laminar or turbulent. Equation 5.16 shows the non-dimensional interfacial shear stress.

$$\tau_i^* = f_i \left[\frac{G_g^2}{2\rho_g} \right] \left[\frac{\rho_f}{(\rho_f - \rho_g)^2 \mu_f^2 g^2} \right] \tag{5.16}$$

With the interfacial shear stress calculated for each of the experiments, the values can be compared with one another. Figure 5.10 shows the relationship between the interfacial shear stress and the inlet steam Reynolds number. The lower curve of two points from Test 6, Steps 4 and 5 are at a lower pressure and represent the two lowest total condensation for all of the tests. The separation is due to the physical properties, mainly the pressure. Test 6 was at a lower pressure which gives a lower Reynolds number. The shape of the curves depend on the Reynolds number and the interfacial shear stress. The combination of lower pressure and higher velocities negate each other for the Reynolds number calculation, but give and increase of interfacial shear stress.

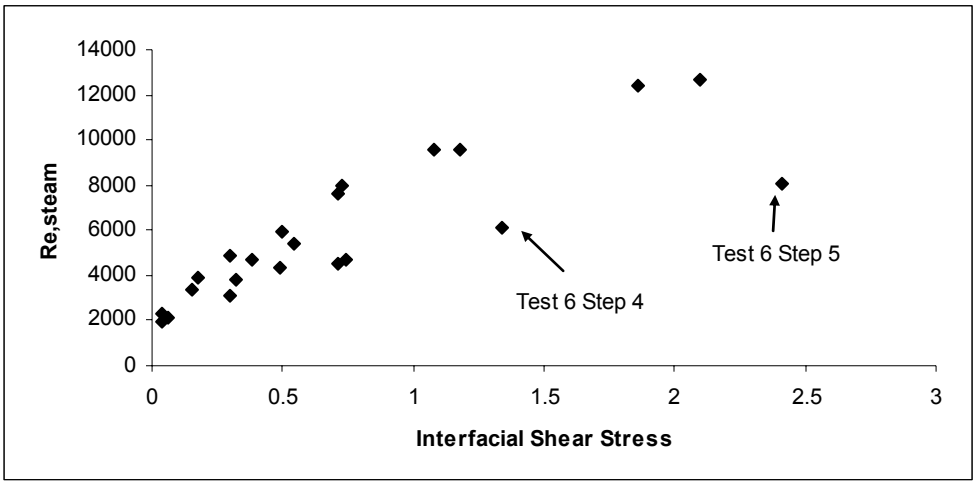

Figure 5.10 – Steam Inlet Reynolds Number vs Interfacial Shear Stress

Figure 5.11 shows the relationship between the interfacial shear stress and the condensate carryover ratio. Since there is only one data point that is greater than one, it is difficult to develop a relationship between the two values.

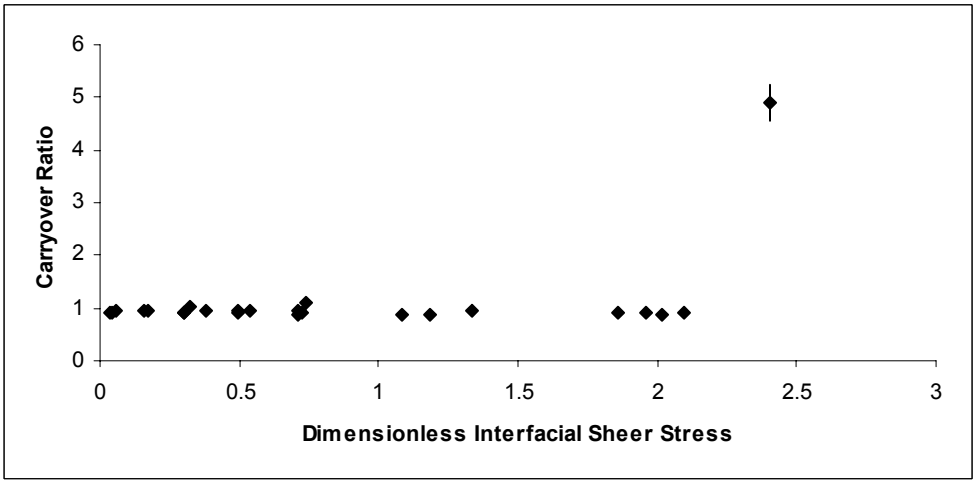

Figure 5.11 – Carryover Ratio versus Interfacial Shear Stress

Since the modified Nusselt number is of importance in determining the heat transfer inside the U-tubes, Figure 5.12 shows the relationship between the

interfacial shear stress and the modified Nusselt number. However, the figure shows there is no discernable relationship between the two. The interfacial shear stress is used to determine the force of the moving steam on the condensate film. In these experiments, the interfacial shear stress was not shown to affect the film except for Test 6 Step 5. Without having a large effect on the film, the modified Nusselt number should not be a function of the shear stress and can be seen in the figure.

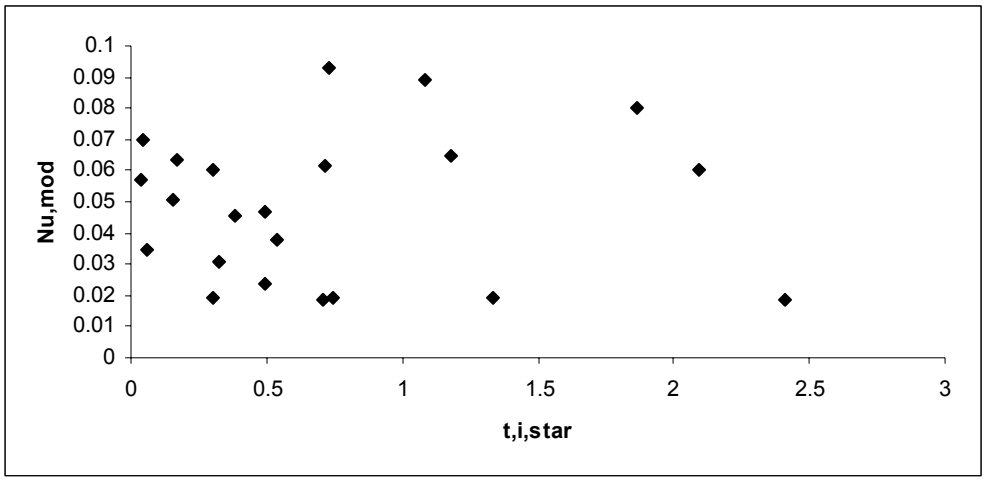

Figure 5.12 – Modified Nusselt Number versus Interfacial Shear Stress

Comparison of Data

The condensation experiments completed using the OSU APEX facilities are unique. As stated in Chapter 2, facilities using a full scale U-tube steam generator for reflux condensation tests were looking at system wide effects of the heat transfer and not steam generator specific phenomena. Other similar experiments involve vertical tubes, and usually no more than ten tubes total. This system has 133 tubes, and that makes these sets of experiments unique.

FLECHT SEASET Comparison

The Nuclear Regulatory Commission working with the Electric Power Research Institute and Westinghouse Electric Corporation developed the Full Length Emergency Cooling Heat Transfer Separate Effects and System Effects Test (FLECHT SEASET) test program. The purpose of this program was to determine the hydraulic and heat transfer phenomena during natural circulation cooling modes (FLECHT SEASET 1984).

The test program included single phase, two phase, and reflux condensation modes of natural circulation cooling. The facility was split into two different loops: the broken loop that represented a single PWR loop, and the unbroken loop that represented three scaled PWR loops.

The facility and types of tests that were performed are comparable to the tests done using the APEX facility, but there are a few major differences that need to be discussed. The FLECHT SEASET facility is a full length, volume scaled facility with a heater power input of 222 kW. The APEX facility was a ¼ length scaled facility with a heater power input that ranged between 200 kW and 1 MW. Also, the secondary sides of the steam generators were at different conditions. For the APEX tests, prior to the start of each step, the steam generator secondary side was filled up and heated to saturation conditions with a pressure that was approximately 0.07 MPa less than the primary side. No new water was added during the step, and at no time did the water fall below the top of the U-tubes. The

process was repeated for the start of each step. Another difference is the flow conditions of the steam inside the U-tubes. For the FLECHT SEASET tests, natural circulation flow was established, giving lower steam inlet velocities. The APEX tests forced steam through the U-tubes, resulting in higher steam velocities.

The FLECHT SEASET tests had a secondary side pressure of 0.28 MPa and subcooled water at approximately 27 degrees Celsius. In order to boil on the secondary side, the water must first be heated to saturated conditions. Subcooled water was added to replace the inventory that was boiled off during the tests. Another difference is that the water level did not fully cover the U-tube bundle. The secondary side water level was approximately ten feet below the top of the U-tube bundle.

The heat transfer from the primary side of the steam generator to the secondary side is similar, but does have some major differences. The heat transfer inside the tubes through the condensation layer should be approximately the same. Both are in the turbulent regime for film Reynolds number, with the APEX range of 50-300 and FLECHT SEASET with the range of 500-700. The heat transfer through the tube walls is also similar. The main difference is the boiling on the outside of the steam generator tubes. For the APEX tests saturated nucleate boiling on the outside of the tube walls was assumed. For the FLECHT SEASET tests, slightly subcooled nucleate boiling is assumed on the secondary side. Table 5.2 shows the differences between FLECHT SEASET and the APEX facility.

Table 5.2 – Differences between FLECHT SEASET and APEX

	Tube S.A.	Tube Thickness	Secondary Press.	
APEX	37.726 m^2	.0254 cm	0.30 - 1.97 MPa	
FLECHT SEASET	9.83 m^2 unbroke - 3.28 m^2 broke	.232 cm	.28 MPa	
	ΔT	**Inside h**	**Tube h**	**Outside h**
APEX	~2-6 deg C	~Same	0.006803	Saturated
FLECHT SEASET	~120-145 deg C	~Same	0.006669	Subcooled

With the two facilities and their respective test procedures being very different, they are difficult to compare. The overall heat transfer coefficient between the two facilities are on the same order of magnitude. An important thing to note is that the condensation rates on the uphill and downhill sides of the steam generators for the individual tests for both facilities were approximately equal.

Flat Plate Analysis

Three correlations are used to model the modified Nusselt number in terms of film Reynolds number. Each correlation represents a different flow regime with Equation 5.17 showing laminar, Equation 5.18 (Kutateladze 1963) showing laminar-wavy, and Equation 5.19 (Labuntsov 1957) showing turbulent.

$$Nu_{\mathrm{mod}} = 1.47 \cdot \mathrm{Re}_{\delta}^{-1/3} \qquad \mathrm{Re}_{\delta} \le 30 \tag{5.17}$$

$$Nu_{\mathrm{mod}} = \frac{\mathrm{Re}_{\delta}}{1.08 \cdot \mathrm{Re}_{\delta}^{1.22} - 5.2} \qquad 30 \le \mathrm{Re}_{\delta} \le 1800 \tag{5.18}$$

$$Nu_{\mathrm{mod}} = \frac{\mathrm{Re}_{\delta}}{8750 + 58 \cdot \mathrm{Pr}_{l}^{-0.5}\left(\mathrm{Re}_{\delta}^{0.75} - 253\right)} \qquad \mathrm{Re}_{\delta} \ge 1800 \tag{5.19}$$

Figure 5.13 shows the above correlations plotted against the experimental data collected. From the figure, it is determined that the flat plate analysis and correlations are not the correct way to model phenomena inside U-tubes.

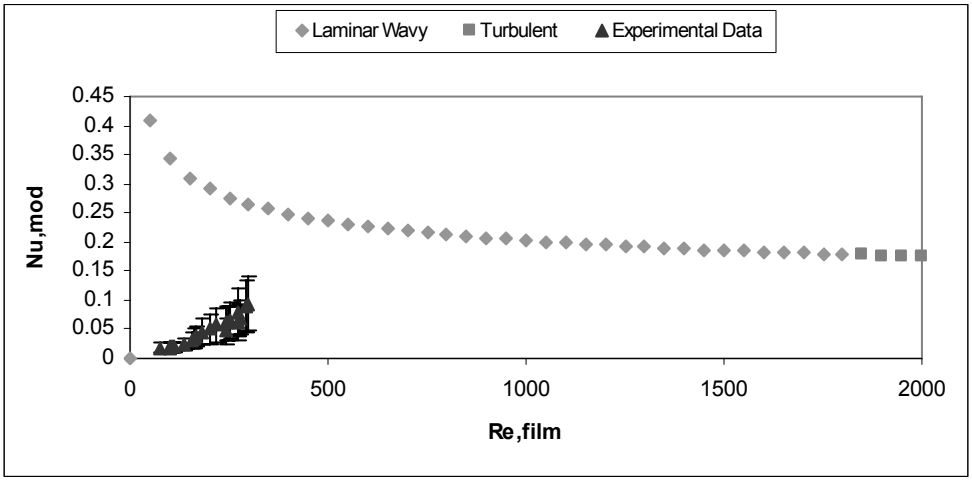

Figure 5.13 – Comparison of Flat Plate Correlations to Experimental Data

As stated above, the data shows that the condensate film is in the turbulent regime, yet for a flat plate the turbulent regime does not show the same upward trend for Reynolds numbers from 500 to 2000. The geometry differences from the flat plate and the U-tubes restrict the use of these correlations to model the experimental data.

Horizontal Tube Analysis

Research conducted by Park, No, and Bang used RELAP5 to model steam condensation inside horizontal tubes. Equation 5.20 shows a correlation used in

the research, but developed by Kim to model heat transfer coefficients (Kim 1983).

$$Nu_{\text{mod}} = 0.966 \times 10^{-3} \cdot \text{Re}_{\delta}^{.98}\, Fr^{.8}\, \text{Pr}_{l}^{.95} \tag{5.20}$$

Figure 5.14 shows the comparison of the Kim correlation to the experimental data collected.

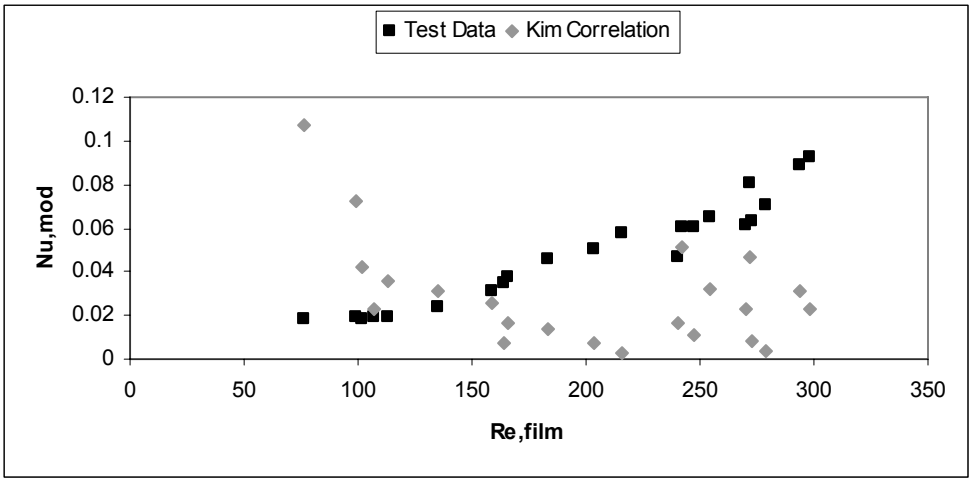

Figure 5.14 – Comparison of Kim Correlation to Experimental Data

Again, this correlation does not accurately depict what is going on inside the steam generator U-tubes; however the data is in the same order of magnitude. The Froude and Prandtl Numbers calculated from the APEX data were used for this correlation so that the Nusselt Number was a function of the film Reynolds Number.

Vertical Tube Analysis

Research conducted by Carpenter and Colburn led to the development of a correlation for modified Nusselt number for condensation inside a vertical tube. Equation 5.21 shows the correlation which was developed for Prandtl numbers ranging from 1.8-2.2 (Carpenter and Colburn 1951).

$$Nu_{\mathrm{mod}} = 0.043 \cdot \mathrm{Pr}_l^{1/2}\, \tau_i^{*1/2} \tag{5.21}$$

Figure 5.15 shows the comparison of the Carpenter and Colburn correlation to the experimental data.

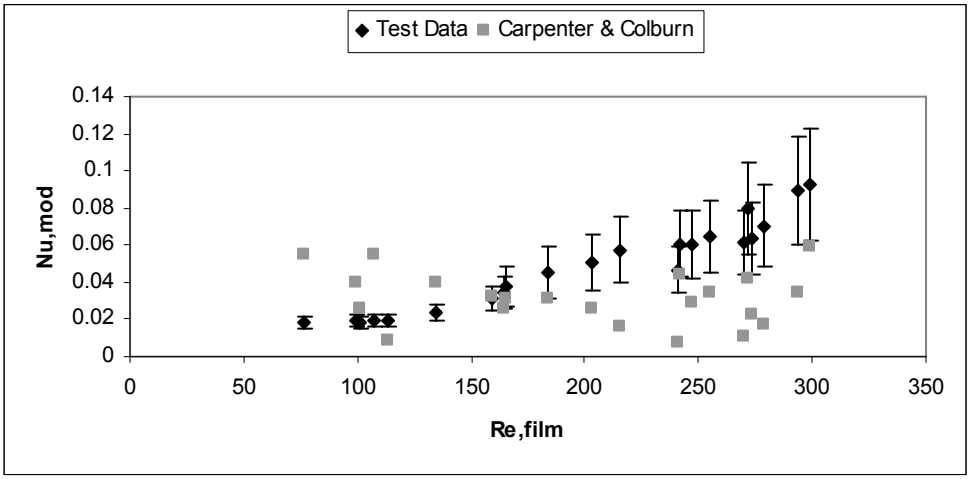

Figure 5.15 – Comparison of Carpenter and Colburn with Experimental Data

The trend looks similar to that of the Kim correlation, but the data is of the same order of magnitude. The error in the test data encompasses the correlation, however the trends are opposite. The correlation shows a decrease of the modified Nusselt number with increasing Reynolds number, while the test data shows the opposite. Since the U-tubes are in a vertical orientation, it makes sense that this

correlation for vertical tubes would be most comparable to the test data; however it does not accurately depict the increase in heat transfer with the increase of film Reynolds number. Reasons for this may include that the Carpenter and Colburn correlation was implemented for interfacial shear stresses between 5 and 150. From the experiments, a maximum value of only 2.5 was obtained which may result in the discrepancy.

Figure 5.16 shows the comparison of the Nusselt number calculated from the tests and a correlation developed by Akers, et al. The correlation uses both the film and steam Reynolds numbers with the density and viscosity ratio. It can be seen in Equation 5.22 (Akers, et al. 1959)

$$Nu = 0.026\,\mathrm{Pr}_l^{0.33}\left(\mathrm{Re}_v\left(\frac{\mu_v}{\mu_l}\right)\left(\frac{\rho_l}{\rho_v}\right)^{0.5} + \mathrm{Re}_l\right)^{0.8} \tag{5.22}$$

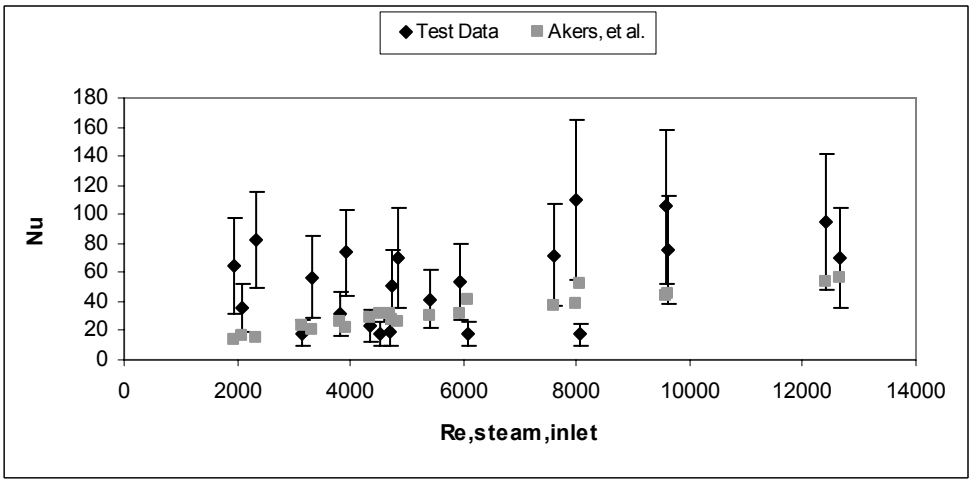

Figure 5.16 – Akers, et al. Correlation Compared to APEX Data

This correlation compares the standard Nusselt number calculated in Equation 5.3. Plugging in the test data into the Akers correlation produces an increasing trend

line similar to the modified Nusselt number trend. The test data was calculated using Equation 5.3 with d being the tube inside diameter. The data is of the same order of magnitude and including the error in calculation, the correlation represents the data well.

Heat Transfer for Reflux Condensation

Even with the comparison to completed work, the main question of whether or not reflux condensation will adequately remove decay heat during a SB-LOCA still remains. In order to determine this, data from a potential new PWR design is used. The EPR which is designed and built by AREVA may incorporate reflux condensation during a SB-LOCA scenario. The EPR operates at 4500 MW_{th} and as stated before, during shutdown will give a maximum decay heat of about 270 MW_{th}. The EPR is a four loop design with four separate steam generators with 5,980 tubes and an outside heat transfer surface area of 7,960m^2 for each steam generator.

To determine if reflux condensation is a viable method data from the EPR and the test data from APEX are compared. The first step is to determine the conditions present for a SB-LOCA scenario in the EPR. If a SB-LOCA occurs, the primary side of the plant depressurizes to 5.5 MPa. The controllers have the ability to control pressure on both the primary and secondary side. The decay heat drops quite rapidly: one second after shutdown the decay heat is six percent of the operating power, 100 seconds gives a decay heat of 3.5%, and 1000 seconds gives 2.25%. Reflux condensation is assumed to not start happening until around 1000

seconds after shutdown. For reflux condensation to occur, multiple safety systems must fail and the liquid inventory must boil to create the steam space in the primary side. Table 5.3 shows the temperature difference needed from the primary side to the secondary side to remove the decay heat after reactor shut down. Different percentages are given that represent periods of time after shutdown.

Table 5.3 – EPR Decay Heat Removal

Operating Power 4500 MW		Number of Tubes 23920		Tube Surface Area 31840 m^2	
Decay Power %	6.00%	3.00%	2.00%	1.00%	0.50%
Decay Power (MW)	270	135	90	45	22.5
Primary Pressure (bar)	55	55	55	55	55
Pr,film	1.489841	1.489841	1.489841	1.489841	1.489841
Re,film	5112.777	2556.388	1704.259	852.1295	426.0647
Nu,mod	3.021137	1.236182	0.732935	0.299901	0.122713
hi (W/m^2-C)	14432.07	5905.283	3501.256	1432.636	586.2031
ho (W/m^2-C)	8428.672	5521.967	4293.649	2761.826	1758.486
U (W/m^2-C)	16.29825	16.2552	16.34081	16.33288	16.31504
delta T ('C)	52.02951	26.08365	17.298	8.653201	4.331331
Secondary Pressure (bar)	22.29405	35.81347	41.58369	47.93069	51.36864

These values assume that the primary side pressure drops to 5.5MPa and is held there. The film Reynolds number is determined by the amount of condensate produced to transfer all of the decay heat to the secondary side. The modified Nusselt number is calculated from APEX data. Assuming saturated boiling on the outside of the tubes and taking into account the heat transfer through the tube wall, the overall heat transfer coefficient is calculated from the modified Nusselt number. Dividing the overall heat transfer coefficient and the surface area into the decay energy gives the temperature difference needed, and from there the secondary side saturation pressure is calculated.

From this analysis it appears as if reflux condensation may adequately remove the decay heat after reactor shutdown from a SB-LOCA. A decay heat of approximately two percent, which is about 20 minutes after shutdown, is a reasonable assumption.

The following equation was used in the analysis of the EPR during reflux condensation after a SB-LOCA. Equation 5.23 is used to measure the modified Nusselt number as a function of the film Reynolds number.

$$Nu_{\text{mod}} = 2.0 \times 10^{-5} \cdot \text{Re}_{\delta}^{1.4714} \tag{5.23}$$

The above equation is used for the turbulent film condensation conditions seen in the APEX tests. Use of the equation outside of the data range may produce inaccurate results.

Chapter 6 – Conclusion

Experiment Summary

The OSU APEX facility was modified from its original state so that the NRC Condensation tests could be performed. Steam Generator 1 was removed from the primary loop piping and dry steam from Steam Generator 2 was piped into the hot leg of SG #1. A cyclone steam separator was added on the downhill side to remove all of the condensate from the steam flow. A catch tank was added on the uphill side to collect the condensate from the hot-leg side.

The six tests conducted at the APEX facility have given experimental data to benchmark computer codes and develop understanding of the phenomena that occurs inside the steam generator. The versatility of the facility has allowed six tests and different pressures ranging from 0.45 MPa to 2.38 MPa. While no correlation was found from other research that correctly predicts the modified Nusselt number or the overall heat transfer coefficient seen in these tests, a trend can be seen for both cases. The following conclusions can be drawn from the experiments:

1. The collapsed liquid level in the catch tank under-predicts the condensation rate on the hot leg side. The expansion as the condensate enters the tank results in some of it flashing to steam. Once the flashed inventory is considered, the condensation rates on both the hot and cold legs are

relatively the same. It should be noted that the hot and cold leg condensation rates for the FLECHT SEASET tests were also the same.

2. The condensate film in the tubes appears to be in the turbulent regime. This is confirmed by the increasing Nusselt number as a function of film Reynolds number for all tests except Test-6. The flow regime seen in Test-6 shows the characteristics of the transition from laminar-wavy to turbulent.
3. The Prandtl number for all of the tests varied from 0.87 to 1.26. While a trend of decreasing Prandtl number resulting in higher Nusselt number was shown, the range of values for the Prandtl number are small and a conclusive relationship between the two cannot be determined.
4. The overall heat transfer coefficient or the modified Nusselt number are not a direct function of the steam inlet Reynolds number, however the use of the Akers, et al. correlation shows a trend within the error of the calculated data
5. The carry-over ratio was one for all but one test. While the heat transfer coefficient is independent of the carry-over ratio, it should be noted that for this set of tests, the lowest total condensation rate was observed when the carry-over ratio was greater than one. Also, the largest interfacial shear stress was observed with the greatest carry-over ratio.
6. The use of reflux condensation as a method of decay heat removal during a SB-LOCA is reasonable. After the reactor is shut down and the system is

depressurized, the amount of time before reflux condensation begins will give a decay heat that can be removed by reflux condensation alone. The temperature differences between the primary and secondary sides can be obtained by lowering the pressure in the secondary side. If the primary side pressure is maintained at 5.5 MPa, a secondary pressure of 4.0 MPa or less would be sufficient in removing the decay heat.

Future Work

The analysis of the experimental data was limited due to no direct observation of what phenomenon was occurring inside the U-tubes. The inside heat transfer coefficient was back calculated and included the use of correlations to determine the heat transfer coefficients on the outside of the tube wall. In order to more accurately depict what is happening inside the U-tubes the tube bundle itself would need more instrumentation. Recommended instrumentation includes: inside and outside tube wall thermocouples, the addition of more fluid thermocouples on the inside and outside of the tubes, and instrumentation to measure the condensate film thickness. Adding new instruments would most likely require a reduction in the number of tubes used, but would give greater information about the phenomena occurring.

With the addition of the extra instrumentation, heat fluxes on the inside and outside of the tube walls can be calculated directly. This reduces the need for the use of correlations to calculate the inside and outside heat transfer coefficient, and

the accuracy of the measurements increases. With more accurate data, the amount of heat that can be transferred using reflux condensation will be more precise leading to more accurate correlations to model the data.

At the start of the experiment, it was assumed that the steam inlet Reynolds number would play a large role in the heat transfer process. The tests were designed to give a large range of Reynolds numbers to determine the heat transfer. After analyzing the data, it was observed that the heat transfer was not a function of the steam inlet Reynolds number. Future tests holding Reynolds number relatively constant while changing other parameters of interest, such as Prandtl number and interfacial shear stress, would show what effect they have on heat transfer in the U-tubes. The data collected during these tests represents a very small part of the phenomena occurring during the condensation of steam in U-tubes. Testing at different conditions can only increase the understanding.

Bibliography

Akers, W. W., and Rosson, H. E., ASME-AIChE 3rd National Heat Transfer Conference, Storrs, Conn., Aug. 1959.

Banerjee, et al., "Reflux condensation and transition to natural circulation in vertical U-tube," Journal of Heat Transfer, Vol. 105, pp. 719-727, 1983.

Bellinghausen, R. and Renz, U., "Heat transfer and film thickness during condensation of steam flowing at high velocity in a vertical pipe," International Journal of Heat and Mass Transfer, Vol. 35, No. 3, pp. 683-689, 1992.

Borishanskiy V. M. et al., "Heat transfer coefficients in steam condensation in a vertical tube," HEAT TRANSFER-Soviet Research, Vol. 13, No. 2, March-April, pp. 52-64, 1981.

Carpenter, F, G., and A. P. Colburn, "The Effect of Vapor Velocity on Condensation Inside Tubes," Proceedings of the General Discussion of Heat Transfer, The Institute of Mechanical Engineers and the ASME, pp. 20-26, July 1951.

Collier, J. G., Convective Boiling and Condensation, Oxford Univ Pr, 1996.

Cooper, M. G., "Heat flow rates in saturated nucleate pool boiling—a wide ranging examination using reduced properties," Advances in Heat Transfer, Academic Press, Orlando, Vol. 16, 157-239, 1984.

FLECHT SEASET, "PWR FLECHT SEASET Systems Effects Natural Circulation and Reflux Condensation," NUREG/CR-3654, 1984.

Girard, R., Chang, J.S., "Reflux condensation phenomena in single Vertical Tubes," Int. J. Heat Mass Transfer. Vol. 35, No.9, pp. 2203-2218, 1992.

Incropera, et al., Fundamentals of Heat and Mass Transfer, John Wiley & Sons inc., 2007.

Jeong, et al., "Thermal-hydraulic phenomena during reflux condensation cooling in steam generator tubes," Ann. Nuclear Energy, Vol. 25, No. 17, pp. 1419-1428, 1998.

Kim K.T., "A semi-empirical heat transfer coefficient for laminar and turbulent film condensation on a vertical surface," Ph.D. Thesis, Korea Advanced Institute of Science and Technology, Korea, 1991.

Kim, S. J. and No, H. C., "Turbulent film condensation of high pressure steam in a vertical tube," International Journal of Heat and Mass Transfer, Vol. 43, pp. 4031-4042, 2000.

Klein S. J. & McClintock, F. A., "Describing Uncertainties in Single-Sample Experiments," Mech. Eng., p. 3, January 1953.

I.L.Kreidin, B.L.Kreodom, V.A.Lokshin, "An Experimental investigation of Local Heat Transfer with Condensation," Thermal Engineering, of Steam inside Vertical Tubes, Vol. 32, No. 11, pp. 641-645, 1985.

Kutateladze, S. S., Fundamentals of Heat Transfer, Academic Press, New York, 1963.

Bibliography (Continued)

Labuntsov, D. A., *Teploenergetika*, Vol. 4, 72, 1957.

Lee, C.J, & Choi, S.Y., "Transient analysis of a condensation experiment in the noncondensable gas-filled closed loop using an inverted U-tube," Ann. Nucl. Energy Vol. 23, No. 14, pp. 1179-1188, 1996.

Liu, T. J., "Reflux condensation behavior in a U-tube Steam generator with or without noncondensables," Nuclear Engineering and Design, Vol. 204, pp. 221–232, 2001.

Lucas, K. and Moser, B., "Laminar Film Condensation of Pure Vapours in Tubes" Int. J. Heat Mass Transfer. Vol. 22, pp. 431-435, 1978.

Narain, A. and Kizilyalli, Y., "Pressure driven flow of pure vapor undergoing laminar film condensation between parallel plates," Int. Journal of Non-Linear Mechanics, Vol. 26, No. 5, pp. 501-520, 1991.

Nusselt, M., "Die Oberflachen Kondensation Des Wasserdampfes," Zeitschrift des Vereines Deutscher Ingeniere, Vol. 60, pp. 541-569, 1916.

Pan, Y., "Condensation characteristics inside a vertical tube considering the presence of mass transfer, vapor velocity and interfacial shear," International Journal of Heat and Mass Transfer, Vol. 44, pp. 4475-4482, 2001

Park H. S., No H. C., & Bang Y. S., "Analysis of experiments for in-tube steam condensation in the presence of noncondensable gases at a low pressure using the RELAP5/MOD3.2 code modified with a non-iterative condensation model," Nuclear Engineering and Design, Vol. 225, No. 2-3, pp. 173-190, November 2003.

Reyes, J. N. and Groome, J. T., "OSU APEX-1000 Test Facility Description Report," 2003.

Rohesnow, W. M., "Heat Transfer and Temperature Distribution in Laminar Film Condensation," Transactions of the ASME, pp. 1645-1648, 1956.

Rohesnow, W. M., et al., "Effect of Vapor Velocity on Laminar and Turbulent Film Condensation," Transactions of the ASME, pp. 1637-1643, 1956.

Seban R. A. and Hodgson J. A., "LAMINAR FILM CONDENSATION IN A TUBE WITH UPWARD VAPOR FLOW," Int. J. Heat Mass Transfer. Vol. 25, No.9, pp. 1291-1300, 1982.

Sparrow, E. M., Gregg, J. L., "A boundary layor treatment of laminar film condensation," ASME Journal of Heat Transfer, pp. 13-18, 1959

Sun, G. Hewitt, G. F., "Evaporation and condensation of steam-water in a vertical tube," Nuclear Engineering and Design, Vol. 207, pp. 137-145, 2001.

Todreas, N. E., & Kazimi, M. S., Nuclear Systems 1 – Thermal Hydraulic Fundamentals, Hemisphere Publishing, 1990.

Ueda et al., "Heat Transfer and Pressure Drop for Flow Condensation Inside a Vertical Tube," JSME, Vol. 15, No. 88, pp. 1267-1277, 1972.

Ueda et al., "Heat transfer from steam condensing inside a vertical tube," International Heat Transfer Conference, pp. 304-308, 1974

APPENDICES

Appendix A – Uncertainty Calculations

Due to the number of instruments in the facility, there is an inherent uncertainty in any measurement. This comes from the fact that there is an uncertainty in the instrument itself and when multiplied, divided, added, or subtracted, the uncertainty of the measurement carries through.

Instrument Uncertainty

For the analysis of the NRC Condensation Tests there is an inherent error when calculating the mass and energy balance of the system due to the uncertainty of the instrument. The instruments used for analysis are flow meters, pressure gages, differential pressure level meters, and thermocouples. Table A1 shows the uncertainty of the flow meters, Table A2 shows the uncertainty of the pressure gages and the DP meters, and Table A3 shows the uncertainty of the thermocouples.

Table A1 – Flow Meter Uncertainty Data

	Span			Total Instrument		DAS Error		Total System Error	
Name	Low	high	CalUnits	% of Flow	gpm/cfm	% of Flow	gpm/cfm	% of Flow	gpm/cfm
FVM-001	0	100	cfm	1.00%	1.00	0.040%	0.040	1.001%	1.001
FVM-002	0	100	cfm	1.00%	1.00	0.040%	0.040	1.001%	1.001
FVM-003	0	140	cfm	1.00%	1.40	0.040%	0.057	1.001%	1.401
FVM-004	0	70	cfm	1.00%	0.70	0.040%	0.028	1.001%	0.701

Table A2 – Pressure and Level Meter Uncertainty Data

	Span			Static Pressure	Total Instrument	DAS Error	Total System Error	
Name	Low	high	CalUnits	psi	% URV		% of URV	psi of URV
PT-002	0	500	psig	400	0.20%	0.04%	0.21%	1.038328
PT-004	0	500	psig	400	0.20%	0.04%	0.21%	1.038328
PT-501	0	500	psig	400	0.20%	0.04%	0.21%	1.038328
								in of URV
DP-217	0	32.72	" H2O	250	0.23%	0.04%	0.23%	0.3519569
DP-219	0	30	" H2O	0	0.17%	0.04%	0.18%	0.2625

Table A3 – Thermocouple Uncertainty Data

Name	Eng Min	Eng Max	Type	Thermocouple	Units	TBX-1303	DAS	Total System
	°F	°F		Accuracy °F		Accuracy °F	% of Reading	Accuracy °F
TF-207	0	1000	Fluid	1.98	°F	0.9	0.04%	2.17
TF-209	0	1000	Fluid	1.98	°F	0.9	0.04%	2.17
TF-211	0	1000	Fluid	1.98	°F	0.9	0.04%	2.17
TF-213	0	1000	Fluid	1.98	°F	0.9	0.04%	2.17
TF-215	0	1000	Fluid	1.98	°F	0.9	0.04%	2.17
TF-217	0	1000	Fluid	1.98	°F	0.9	0.04%	2.17

Uncertainty Methodology

For each test and step a mass and energy balance is completed for the system. In order to calculate the mass and energy uncertainty, the uncertainty of the instruments used needs to be considered in the analysis. Klein and McClintock developed a method for calculating uncertainties and their methods are used below. Equation A.1 below shows the calculation of mass from the flow meter data. Density is determined from saturated steam tables at the pressure measured

by the pressure gage. There is assumed to be no error in the correlation determining density.

$$Mass = \dot{V} \cdot \rho \cdot t \tag{A.1}$$

Equation A.2 below shows the calculation of mass in the catch tank and separator tank using the level meters. The areas of the tanks remain constant and again, the density is determined from the saturated pressure conditions.

$$Mass = A \cdot height \cdot \rho \tag{A.2}$$

For the mass determined by the flow meter, the mass is a function of flow, density, and time. The uncertainty of flow and density can be determined from the data in Tables A1 & A2, and the time has no uncertainty associated with it.

$$Mass = f(\dot{V}, \rho, t) \tag{A.3}$$

Equation A.3 shows mass as a function of volumetric flow rate, density, and time. Let w_M be the uncertainty of the result, with $w_{V,}$ w_ρ, and w_t be the uncertainties in the respective variables. Thus the uncertainty of the result is given by Equation A.4 (Klein & McClintock 1953).

$$w_M = \left[\left(\frac{\delta M}{\delta \dot{V}} w_{\dot{V}} \right)^2 + \left(\frac{\delta M}{\delta \rho} w_\rho \right)^2 + \left(\frac{\delta M}{\delta t} w_t \right)^2 \right]^{1/2} \tag{A.4}$$

To determine the mass uncertainty for the level measurement, the same procedure is followed but flow rate and time are replaced with height and area.

Table A4 below shows an example of the mass balance taken from Condensation Test 5, Step 4. The Density of the vapor and liquid was calculated using Steam Tab.

Table A4– Test 5 Step 4 Mass Uncertainties

	Mass = Flow-rate * Density * time							
	lbm	wp	+-		min	observed	max	+-
Steam In FVM-002	429.5772596	0.010567354	4.539495		425.0377646	429.5772596	434.11675	4.539495
Steam out FVM-001	341.6767943	0.010574184	3.612953		338.063841	341.6767943	345.28975	3.612953
Steam out FVM-003	71.06469275	0.010615445	0.754383		70.31030944	71.06469275	71.819076	0.754383
Steam out FVM-004	10.12590004	0.010008157	0.101342		10.02455844	10.12590004	10.227242	0.101342
	Mass = Area* deltah * Density							
	lbm	wp	+-					
Liquid from Sep	34.59371135	0.034893098	1.207082		33.38662959	34.59371135	35.800793	1.207082
Liquid from Catch	31.0459336	0.032767445	1.017296		30.02863768	31.0459336	32.06323	1.017296
			+-	Steam In	% Error			
			6.013539	429.5773	0.013998737			

The energy uncertainty calculations follow the same path only enthalpy is added to the formula. Energy calculated from steam flow through the flow meter is given in Equation A.5

$$Energy = \dot{V} \cdot \rho \cdot h \cdot t \tag{A.5}$$

The uncertainty for the energy is calculated in Equation A.6 by the same was as the mass except with the added enthalpy term.

$$w_E = \left[\left(\frac{\delta E}{\delta \dot{V}} w_{\dot{V}} \right)^2 + \left(\frac{\delta E}{\delta \rho} w_\rho \right)^2 + \left(\frac{\delta E}{\delta t} w_t \right)^2 + \left(\frac{\delta E}{\delta h} w_h \right)^2 \right]^{1/2} \tag{A.6}$$

Table A5 below shows the energy uncertainty for Test 5 Step 4.

Table A5 – Test 5 Step 4 Energy Uncertainties

Energy = Flow Rate * Density * Enthalpy * 60/ 3412								
	KW	wp	+-		min	observed	max	+-
Steam In FVM-002	909.0173	0.01056738	9.605932		899.4114	909.0172983	918.6232	9.605932416
Steam out FVM-001	722.98	0.01057421	7.644944		715.3351	722.9800076	730.625	7.644944181
Steam out FVM-003	150.3292	0.01061548	1.595817		148.7334	150.3292444	151.9251	1.595817022
Steam out FVM-004	20.48226	0.01000816	0.20499		20.27727	20.48225808	20.68725	0.204989664
Energy = Area * deltah * Density * Enthalpy * 6/3412								
	KW	wp	+-					
Liquid from Sep	23.92481	0.03490439	0.835081		23.08973	23.92481042	24.75989	0.835080818
Liquid from Catch	9.836592	0.03276744	0.32232		9.514272	9.836591573	10.15891	0.322319971
			+-		Steam In	% Error		
			12.41407		909.0173	1.37%		

Figure A1 below shows the mass and energy uncertainties for each of the tests and steps. The energy and mass balances are between one and three percent and is acceptable for the facility.

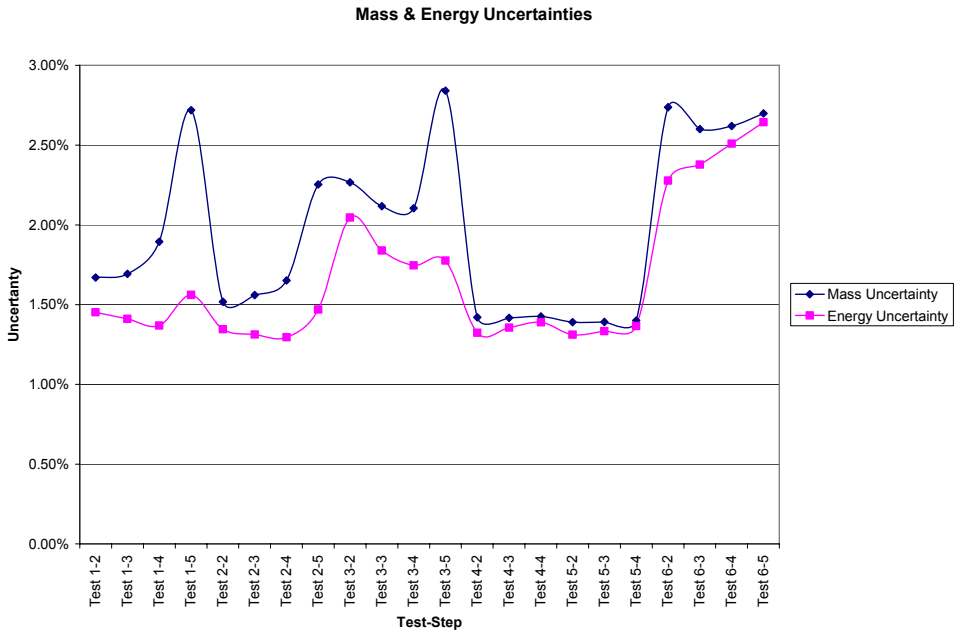

Figure A1 – Mass and Energy Uncertainties

Appendix B – Test Mass and Energy Balances

NRC-Condensation-001

Step-2

Table B1 – Test 1 Step 2 Mass and Energy Balance

Mass Balance		
Steam Mass in	81.204	kg
Steam Mass out Sep	(58.904)	kg
Steam Mass out Ckt	(1.700)	kg
Condensation in Sep	(11.039)	kg
Condensation in Ckt	(9.939)	kg
Difference	(0.377)	
Error	-0.465%	

Energy Balance		
Steam Energy in	377.030	KW
Steam Energy out Sep	(273.400)	KW
Steam Energy out Ckt	(0.064)	KW
Steam Energy out SG	(91.291)	KW
Condensation Energy Sep	(14.812)	KW
Condensation Energy Ckt	(6.942)	KW
Difference	(9.479)	
Error	-2.514%	

Step-3

Table B2 – Test 1 Step 3 Mass and Energy Balance

Mass Balance		
Steam Mass in	71.248	kg
Steam Mass out Sep	(46.582)	kg
Steam Mass out Ckt	(1.892)	kg
Condensation in Sep	(12.192)	kg
Condensation in Ckt	(10.763)	kg
Difference	(0.181)	
Error	-0.254%	

Energy Balance		
Steam Energy in	330.967	KW
Steam Energy out Sep	(216.347)	KW
Steam Energy out Ckt	(0.438)	KW
Steam Energy out SG	(96.967)	KW
Condensation Energy Sep	(16.574)	KW
Condensation Energy Ckt	(7.518)	KW
Difference	(6.878)	
Error	-2.078%	

Step-4

Table B3 – Test 1 Step 4 Mass and Energy Balance

Mass Balance		
Steam Mass in	50.116	kg
Steam Mass out Sep	(22.473)	kg
Steam Mass out Ckt	(1.159)	kg
Condensation in Sep	(13.117)	kg
Condensation in Ckt	(11.735)	kg
Difference	1.632	
Error	3.257%	

Energy Balance		
Steam Energy in	232.983	KW
Steam Energy out Sep	(104.469)	KW
Steam Energy out Ckt	(5.167)	KW
Steam Energy out SG	(104.944)	KW
Condensation Energy Sep	(18.198)	KW
Condensation Energy Ckt	(8.197)	KW
Difference	(7.992)	
Error	-3.430%	

Step-5

Table B4 – Test 1 Step 5 Mass and Energy Balance

Mass Balance		
Steam Mass in	29.192	kg
Steam Mass out Sep	(0.059)	kg
Steam Mass out Ckt	(1.692)	kg
Condensation in Sep	(13.383)	kg
Condensation in Ckt	(12.525)	kg
Difference	1.533	
Error	5.250%	

Energy Balance		
Steam Energy in	135.782	KW
Steam Energy out Sep	(0.273)	KW
Steam Energy out Ckt	(7.547)	KW
Steam Energy out SG	(111.057)	KW
Condensation Energy Sep	(18.828)	KW
Condensation Energy Ckt	(8.748)	KW
Difference	(10.671)	
Error	-7.859%	

NRC-Condensation-002

Step-2

Table B5 – Test 2 Step 2 Mass and Energy Balance

Mass Balance		
Steam Mass in	91.745	kg
Steam Mass out Sep	(61.495)	kg
Steam Mass out Ckt	(2.627)	kg
Condensation in Sep	(14.727)	kg
Condensation in Ckt	(13.042)	kg
Difference	(0.145)	
Error	-0.159%	

Energy Balance		
Steam Energy in	427.400	KW
Steam Energy out Sep	(286.432)	KW
Steam Energy out Ckt	(2.259)	KW
Steam Energy out SG	(116.271)	KW
Condensation Energy Sep	(21.442)	KW
Condensation Energy Ckt	(9.109)	KW
Difference	(8.114)	
Error	-1.899%	

Step-3

Table B6 – Test 2 Step 3 Mass and Energy Balance

Mass Balance		
Steam Mass in	75.069	kg
Steam Mass out Sep	(42.454)	kg
Steam Mass out Ckt	(1.309)	kg
Condensation in Sep	(14.829)	kg
Condensation in Ckt	(13.265)	kg
Difference	3.212	
Error	4.279%	

Energy Balance		
Steam Energy in	349.854	KW
Steam Energy out Sep	(197.839)	KW
Steam Energy out Ckt	(5.838)	KW
Steam Energy out SG	(107.000)	KW
Condensation Energy Sep	(21.893)	KW
Condensation Energy Ckt	(9.265)	KW
Difference	8.018	
Error	2.292%	

Step-4

Table B7 – Test 2 Step 4 Mass and Energy Balance

Mass Balance		
Steam Mass in	61.092	kg
Steam Mass out Sep	(25.836)	kg
Steam Mass out Ckt	(3.888)	kg
Condensation in Sep	(16.445)	kg
Condensation in Ckt	(14.314)	kg
Difference	0.610	
Error	0.998%	

Energy Balance		
Steam Energy in	284.797	KW
Steam Energy out Sep	(120.436)	KW
Steam Energy out Ckt	(17.337)	KW
Steam Energy out SG	(128.801)	KW
Condensation Energy Sep	(24.520)	KW
Condensation Energy Ckt	(9.998)	KW
Difference	(16.295)	
Error	-5.722%	

Step-5

Table B8 – Test 2 Step 5 Mass and Energy Balance

Mass Balance		
Steam Mass in	36.140	kg
Steam Mass out Sep	(0.078)	kg
Steam Mass out Ckt	(4.144)	kg
Condensation in Sep	(16.248)	kg
Condensation in Ckt	(14.662)	kg
Difference	1.008	
Error	2.789%	

Energy Balance		
Steam Energy in	168.534	KW
Steam Energy out Sep	(0.364)	KW
Steam Energy out Ckt	(18.477)	KW
Steam Energy out SG	(136.016)	KW
Condensation Energy Sep	(24.528)	KW
Condensation Energy Ckt	(10.241)	KW
Difference	(21.093)	
Error	-12.515%	

NRC-Condensation-003

Step-2

Table B9 – Test 3 Step 2 Mass and Energy Balance

Mass Balance		
Steam Mass in	67.821	kg
Steam Mass out Sep	(47.719)	kg
Steam Mass out Ckt	(0.918)	kg
Condensation in Sep	(10.144)	kg
Condensation in Ckt	(8.513)	kg
Difference	0.527	
Error	0.776%	

Energy Balance		
Steam Energy in	311.138	KW
Steam Energy out Sep	(218.513)	KW
Steam Energy out Ckt	(4.094)	KW
Steam Energy out SG	(83.425)	KW
Condensation Energy Sep	(10.783)	KW
Condensation Energy Ckt	(5.946)	KW
Difference	(11.623)	
Error	-3.736%	

Step-3

Table B10 – Test 3 Step 3 Mass and Energy Balance

Mass Balance		
Steam Mass in	61.803	kg
Steam Mass out Sep	(34.639)	kg
Steam Mass out Ckt	(1.896)	kg
Condensation in Sep	(10.710)	kg
Condensation in Ckt	(10.681)	kg
Difference	3.878	
Error	6.275%	

Energy Balance		
Steam Energy in	283.926	KW
Steam Energy out Sep	(158.961)	KW
Steam Energy out Ckt	(8.453)	KW
Steam Energy out SG	(94.987)	KW
Condensation Energy Sep	(11.782)	KW
Condensation Energy Ckt	(7.460)	KW
Difference	2.283	
Error	0.804%	

Step-4

Table B11 – Test 3 Step 4 Mass and Energy Balance

Mass Balance		
Steam Mass in	54.084	kg
Steam Mass out Sep	(24.898)	kg
Steam Mass out Ckt	(3.108)	kg
Condensation in Sep	(13.144)	kg
Condensation in Ckt	(11.410)	kg
Difference	1.524	
Error	2.818%	

Energy Balance		
Steam Energy in	248.778	KW
Steam Energy out Sep	(114.460)	KW
Steam Energy out Ckt	(13.857)	KW
Steam Energy out SG	(105.058)	KW
Condensation Energy Sep	(14.868)	KW
Condensation Energy Ckt	(7.970)	KW
Difference	(7.436)	
Error	-2.989%	

Step-5

Table B12 – Test 3 Step 5 Mass and Energy Balance

Mass Balance		
Steam Mass in	29.615	kg
Steam Mass out Sep	(0.018)	kg
Steam Mass out Ckt	(4.841)	kg
Condensation in Sep	(12.517)	kg
Condensation in Ckt	(11.491)	kg
Difference	0.748	
Error	2.526%	

Energy Balance		
Steam Energy in	136.560	KW
Steam Energy out Sep	(0.083)	KW
Steam Energy out Ckt	(21.587)	KW
Steam Energy out SG	(100.311)	KW
Condensation Energy Sep	(14.877)	KW
Condensation Energy Ckt	(8.026)	KW
Difference	(8.324)	
Error	-6.096%	

NRC-Condensation-004

Step-2

Table B13 – Test 4 Step 2 Mass and Energy Balance

Mass Balance		
Steam Mass in	118.574	kg
Steam Mass out Sep	(80.626)	kg
Steam Mass out Ckt	(4.052)	kg
Condensation in Sep	(15.381)	kg
Condensation in Ckt	(14.576)	kg
Difference	3.939	
Error	3.322%	

Energy Balance		
Steam Energy in	552.939	KW
Steam Energy out Sep	(375.973)	KW
Steam Energy out Ckt	(18.070)	KW
Steam Energy out SG	(140.198)	KW
Condensation Energy Sep	(23.184)	KW
Condensation Energy Ckt	(10.181)	KW
Difference	(14.667)	
Error	-2.652%	

Step-3

Table B14 – Test 4 Step 3 Mass and Energy Balance

Mass Balance		
Steam Mass in	149.324	kg
Steam Mass out Sep	(112.225)	kg
Steam Mass out Ckt	(4.011)	kg
Condensation in Sep	(14.533)	kg
Condensation in Ckt	(13.915)	kg
Difference	4.640	
Error	3.108%	

Energy Balance		
Steam Energy in	696.176	KW
Steam Energy out Sep	(523.196)	KW
Steam Energy out Ckt	(17.884)	KW
Steam Energy out SG	(135.758)	KW
Condensation Energy Sep	(21.729)	KW
Condensation Energy Ckt	(9.720)	KW
Difference	(12.111)	
Error	-1.740%	

Step-4

Table B15 – Test 4 Step 4 Mass and Energy Balance

Mass Balance		
Steam Mass in	196.171	kg
Steam Mass out Sep	(158.585)	kg
Steam Mass out Ckt	(4.147)	kg
Condensation in Sep	(14.335)	kg
Condensation in Ckt	(13.112)	kg
Difference	5.993	
Error	3.055%	

Energy Balance		
Steam Energy in	914.266	KW
Steam Energy out Sep	(739.029)	KW
Steam Energy out Ckt	(18.491)	KW
Steam Energy out SG	(130.238)	KW
Condensation Energy Sep	(21.170)	KW
Condensation Energy Ckt	(9.158)	KW
Difference	(3.821)	
Error	-0.418%	

NRC-Condensation-005

Step-2

Table B16 – Test 5 Step 2 Mass and Energy Balance

Mass Balance		
Steam Mass in	125.795	kg
Steam Mass out Sep	(85.059)	kg
Steam Mass out Ckt	(4.320)	kg
Condensation in Sep	(16.849)	kg
Condensation in Ckt	(15.279)	kg
Difference	4.288	
Error	3.409%	

Energy Balance		
Steam Energy in	587.041	KW
Steam Energy out Sep	(396.940)	KW
Steam Energy out Ckt	(19.262)	KW
Steam Energy out SG	(160.931)	KW
Condensation Energy Sep	(26.097)	KW
Condensation Energy Ckt	(10.672)	KW
Difference	(26.862)	
Error	-4.576%	

Step-3

Table B17 – Test 5 Step 3 Mass and Energy Balance

Mass Balance		
Steam Mass in	150.746	kg
Steam Mass out Sep	(110.811)	kg
Steam Mass out Ckt	(4.382)	kg
Condensation in Sep	(16.456)	kg
Condensation in Ckt	(15.351)	kg
Difference	3.746	
Error	2.485%	

Energy Balance		
Steam Energy in	703.390	KW
Steam Energy out Sep	(517.041)	KW
Steam Energy out Ckt	(19.540)	KW
Steam Energy out SG	(156.062)	KW
Condensation Energy Sep	(25.343)	KW
Condensation Energy Ckt	(10.723)	KW
Difference	(25.320)	
Error	-3.600%	

Step-4

Table B18 – Test 5 Step 4 Mass and Energy Balance

Mass Balance		
Steam Mass in	194.853	kg
Steam Mass out Sep	(154.982)	kg
Steam Mass out Ckt	(4.593)	kg
Condensation in Sep	(15.691)	kg
Condensation in Ckt	(14.082)	kg
Difference	5.504	
Error	2.825%	

Energy Balance		
Steam Energy in	908.981	KW
Steam Energy out Sep	(722.951)	KW
Steam Energy out Ckt	(20.481)	KW
Steam Energy out SG	(150.323)	KW
Condensation Energy Sep	(23.924)	KW
Condensation Energy Ckt	(9.836)	KW
Difference	(18.535)	
Error	-2.039%	

NRC-Condensation-006

Step-2

Table B19 – Test 6 Step 2 Mass and Energy Balance

Mass Balance		
Steam Mass in	42.226	kg
Steam Mass out Sep	(22.502)	kg
Steam Mass out Ckt	(1.651)	kg
Condensation in Sep	(9.213)	kg
Condensation in Ckt	(9.264)	kg
Difference	(0.404)	
Error	-0.956%	

Energy Balance		
Steam Energy in	192.986	KW
Steam Energy out Sep	(102.832)	KW
Steam Energy out Ckt	(7.361)	KW
Steam Energy out SG	(81.519)	KW
Condensation Energy Sep	(9.489)	KW
Condensation Energy Ckt	(6.471)	KW
Difference	(14.685)	
Error	-7.610%	

Step-3

Table B20 – Test 6 Step 3 Mass and Energy Balance

Mass Balance		
Steam Mass in	61.270	kg
Steam Mass out Sep	(42.304)	kg
Steam Mass out Ckt	(2.157)	kg
Condensation in Sep	(8.941)	kg
Condensation in Ckt	(8.795)	kg
Difference	(0.927)	
Error	-1.513%	

Energy Balance		
Steam Energy in	279.871	KW
Steam Energy out Sep	(193.174)	KW
Steam Energy out Ckt	(9.620)	KW
Steam Energy out SG	(78.358)	KW
Condensation Energy Sep	(9.098)	KW
Condensation Energy Ckt	(6.143)	KW
Difference	(16.522)	
Error	-5.904%	

Step-4

Table B21 – Test 6 Step 4 Mass and Energy Balance

Mass Balance		
Steam Mass in	82.526	kg
Steam Mass out Sep	(62.179)	kg
Steam Mass out Ckt	(0.695)	kg
Condensation in Sep	(9.034)	kg
Condensation in Ckt	(8.670)	kg
Difference	1.949	
Error	2.361%	

Energy Balance		
Steam Energy in	376.686	KW
Steam Energy out Sep	(283.602)	KW
Steam Energy out Ckt	(1.524)	KW
Steam Energy out SG	(83.137)	KW
Condensation Energy Sep	(9.033)	KW
Condensation Energy Ckt	(6.056)	KW
Difference	(6.665)	
Error	-1.769%	

Step-5

Table B22 – Test 6 Step 5 Mass and Energy Balance

Mass Balance		
Steam Mass in	112.590	kg
Steam Mass out Sep	(78.817)	kg
Steam Mass out Ckt	(2.872)	kg
Condensation in Sep	(12.156)	kg
Condensation in Ckt	(2.329)	kg
Ambient Losses		
Difference	16.416	
Error	14.580%	

Energy Balance		
Steam Energy in	513.190	KW
Steam Energy out Sep	(358.436)	KW
Steam Energy out Ckt	(12.805)	KW
Steam Energy out SG	(80.202)	KW
Condensation Energy Sep	(11.617)	KW
Condensation Energy Ckt	(1.627)	KW
Difference	48.502	
Error	9.451%	